Stony Brook University

Characterization of Rv3545c from *Mycobacterium tuberculosis* and Labeling Wild-Type Cholesterol Oxidase with ^{2}H, ^{13}C, and ^{15}N for Structural Characterization

A Thesis Presented

by

Yoo-Jin Ghang

to

The Graduate School

in Partial Fulfillment of the

Requirements

for the Degree of

Master of Science

in

Chemistry

Stony Brook University

August 2008

Stony Brook University

The graduate School

Yoo-Jin Ghang

We, the thesis committee for the above candidate for the

Master of Science degree, hereby recommend

acceptance of this thesis.

Nicole S. Sampson – Thesis Advisor, Professor, Department of Chemistry

Elizabeth M. Boon – Chairperson of Defense, Assistant Professor, Department of Chemistry

Erwin London – Third member of Defense, Professor, Department of Biochemistry and Cell Biology

This thesis is accepted by the Graduate School

Lawrence Martin
Dean of the Graduate School

Abstract of the Thesis

Characterization of Rv3545c from *Mycobacterium tuberculosis* and Labeling Wild-Type Cholesterol Oxidase with ^{2}H, ^{13}C, and ^{15}N for Structural Characterization

by

Yoo-Jin Ghang

Master of Science

in

Chemistry

Stony Brook University

2008

Mycobacterium tuberculosis (M. tb) is a gram-positive bacterium that causes tuberculosis in humans and more than 30% of the world's population suffers from tubercle bacilli infection. Tuberculosis is extremely dangerous in individuals with HIV-AIDS and a new approach for treating the disease is necessary due to the emergence of multi-drug resistant and extreme-drug resistant. During an infection, *M. tb* targets macrophages, and the utilization of cholesterol was observed to be necessary for *M. tb* to enter and survive in a macrophage. One postulate for the function of cholesterol in *M. tb* is the metabolism of cholesterol to form sterol hormones. Mammals are able to

biosynthesize cortisol that modulates the immune system from cholesterol. The degradation of cholesterol to corticosteroids requires several P450 enzymes and twenty *M. tb* genes have been annotated as P450s, most of which have not been characterized. The operon, *Rv3540c-Rv3545c*, contains the *cyp125* gene which has been shown to be up-regulated in macrophages and is required for survival in macrophages. Microarray analysis and qrt-PCR data revealed that the genes in the operon are induced by cholesterol. To identify the correlation between cholesterol metabolism and the operon in *M. tb*, *cyp125* was expressed in *Escherichia coli* and *Mycobacterium smegmatis* for biochemical characterization.

ChoA is a cholesterol oxidase, secreted by *Streptomyces sp.* SA-COO to degrade steroids into an ingestible carbon source. It is a monomeric enzyme whose molecular weight is 57 kDa. ChoA is a water-soluble flavoenzyme that catalyzes two reactions in one active site: oxidation of cholesterol to cholest-5-en-3-one and isomerization to cholest-4-en-3-one, a more thermodynamically stable product. During the oxidation, a noncovalently bound flavine adenine dinucleotide (FAD) cofactor is reduced to $FADH^-$ and the reduced cofactor is cycled back to the oxidized state by reduction of molecular oxygen to hydrogen peroxide. There are two substrate binding loops: residues 78-87 form loop 1 and residues 433-436 are loop 2. These loops are flexible allowing ChoA to make conformational changes during its catalytic cycle. These loops cap the active site of the protein and it is postulated that a hydrophobic pathway is formed between the active site and the membrane by opening the loops. WT ChoA was labeled with ^{15}N, ^{13}C, and ^{2}H, in order to utilize NMR to study the dynamics of this protein and to interrogate its membrane bound structure.

Table of Contents

Chapter 3

Introduction of Cholesterol Oxidase

Chapter 4

Labeling Wild-Type Choelsterol Oxidase with ^{2}H, ^{13}C, and ^{15}N for Structural Characterization

List of Figures

Chapter 3

Chapter 4

labeled WT ChoA

List of Tables

List of Scheme

List of Abbreviations

2XYT	2Xyeast-tryptone broth
3β-HSD	3β-hydroxysteroid dehydrogenase
Arg	arginine
Asn	asparagine
BSA	bovine serum albumin
ChoA	cholesterol oxidase from *Streptomyces*
ChoE	cholesterol oxidase from *Rhodococcus equi*
CIP	calf intestinal alkaline phosphatase
CoA	coenzyme A
CYP	cytochrome P450
DDI H_2O	distilled, deionized water
DEAE	diethylaminoethyl
DNA	deoxyribonucleic acid
E. coli	*Escherichia coli*
FAD	flavin adenine dinucleotide
FPLC	fast protein liquid chromatography
Glu	glutamic acid
GMC	glucose-methanol-choline
His	histidine
HSQC	heteronuclear single quantum coherence
IPTG	isopropyl-β-D-thiogalactopyranoside

L	liter
LB	Luria broth
Lys	lysine
M. smeg	*Mycobacterium smegmatis*
M. tb	*Mycobacterium tuberculosis*
MWCO	molecular weight cut-off
NAD	nicotinamide adenine dinucleotide
NMR	nuclear magnetic resonance
ORF	open reading frame
PCR	polymerase chain reaction
PDIM	phthiocerol dimycocerosate
PMSF	phenylmethanesulphonylfluoride
POPC	1-palmitoyl-2-oleoyl-sn-glycero-3-phosphochlorine
qrt-PCR	quantitative real time polymerase chain reaction
R. equi	*Rhodococcus equi*
SDS-PAGE	sodium dodecyl sulfate polyacrylamide gel eletrophoresis
TB	tuberculosis
TROSY	Transverse Relaxation-Optimized Spectroscopy
UV	Ultraviolet
Wat	water molecule
WT	wild-type

CHAPTER 1

Introduction of *Mycobacterium tuberculosis* and its Cholesterol Metabolism

I. ***Mycobacterium tuberculosis***

1. **Tuberculosis**
2. ***Mycobacterium tuberculosis***

II. **Cholesterol metabolism in *Mycobacterium tuberculosis***

1. **Primary metabolism of cholesterol**
2. **The disorder in a host membrane**
3. **Secondary metabolism of cholesterol**
4. **Detoxification by cholesterol degradation**

I. *Mycobacterium tuberculosis*

1. Tuberculosis

Tuberculosis (TB), caused by *Mycobacterium tuberculosis* (*M. tb*), is a lethal infectious disease commonly contagious through the air. Over one-third of the world's population suffers from tubercle bacilli infection (*1*) and 5-10 % of these individuals become ill at some point during their life. According to the estimate of the World Health Organization (WHO), 1.6 million people died from TB in 2005 (*2*). The development of TB is boosted by co-infection with the HIV-AIDS virus. The human immune system is weakened by HIV-AIDS and the proliferation of TB becomes out of control. Moreover, the emergence of multidrug-resistant TB (MDR-TB) and extremely drug-resistant TB (XDR-TB) that are resistant to the two most powerful anti-TB drugs (isoniazid and rifampicin) (*3-6*) categorizes TB as a fatal disease which causes human mortality these days. To combat the organisms, new approaches are needed (*7-9*).

2. *Mycobacterium tuberculosis*

Mycobacterium tuberculosis (*M. tb*) is a large rod-shaped gram-positive bacterium that causes tuberculosis in humans. It is an intracellular, slow growing bacterium with a lipid-rich cell wall that targets the macrophages of its host. Macrophages typically engulf pathogens by endocytosis forming a phagosome. The phagosome then fuses to the lysosome, which contains digestive enzymes allowing the macrophage to kill the pathogen. The dead digested pathogens are released from the macrophages. However, *M. tb* follows a different pathway from other pathogens. *M. tb* is also endocytosed by macrophages like other bacteria, but the macrophages are not able to defend against this pathogen. The undestroyable *M. tb* in the phagosome of the macrophage can change its vacuolar environment extensively, preventing acidification and the fusion of the phagosome to the lysosome (*10, 11*). The macrophage phagosome infected with *M. tb* is able to retain tryptophan-aspartate-containing coat (TACO) protein and this ability of mycobacterial phagosome prevents the maturation of the phagosome-lysosome fusion (*12*). Finally, *M. tb* persists intracellularly where it replicates and can lay dormant. The bacteria are then released from the macrophage by disrupting it.

Even though tuberculosis is one of the most prevalent and fatal infectious diseases, the mechanism of *M. tb* pathogenesis is still not clearly known. About 10 years ago, Cole and co-workers determined the sequence of the *M. tb* genome (*13*) and it contains approximately 4,000 open reading frames (ORF). In addition, a large part of the genome is encoding proteins related to lipid synthesis and metabolism.

II. Cholesterol metabolism in *Mycobacterium tuberculosis*

M. tb is an agent that causes tuberculosis in humans and it is especially dangerous in individuals who are infected with HIV due to the weak immune system. During infection *M. tb* is engulfed in immune cells called macrophages, and it is resistant to innate macrophage defenses. Here, the noticeable facts are that cholesterol is associated with the entry of *M. tb* into macrophages and the survival of *M. tb* there (*14*) and the persistence of *M. tb* requires cholesterol uptake in vivo (*15*). In addition, there are several ORFs in the *M. tb* genome that are predicted to encode enzymes related to cholesterol metabolism (*13*). The exit of *M. tb* in the early phagolysosome and the cytosol entry were recently observed by using new electron microscopy techniques (*16*). This result supports that *M. tb* can only reside in early phagosome states and cholesterol degradation might be involved in the disruption of the phagolysosomal membrane.

The exact function of cholesterol degradation has not been demonstrated yet, but there are several possible functions for *M. tb* survival in the mammalian host. *M. tb* might be able to utilize cholesterol as a carbon source and cholesterol degradation may disrupt the eukaryotic host membrane. Also, the host immune response may be down-regulated by the secondary metabolism of cholesterol to steroid hormones. In addition, detoxification can be carried out by cholesterol degradation.

1. Primary metabolism of cholesterol

Enzymes that degrade cholesterol have been indentified in some actinomycete strains and there is a proposed pathway of cholesterol degradation based on their chemical identification (Scheme 1-1) (*17*). The final products of the metabolism pathway of cholesterol in *Rhodococcus* and *Streptomyces* are acetyl CoA and the propionyl CoA that could enter the glyoxalate shunt and be converted to succinate. Only a few genes involved in the individual steps have been identified and most of the enzymes have not been characterized yet. The enzymes categorizing the first step in the pathway have been identified. A cholesterol oxidase is utilized by *Rhodococcus* and *Streptomyces* and it catalyzes two reactions: the oxidation of cholesterol to cholest-5-en-3-one and the isomerization of the intermediate to cholest-4-en-3-one. Then, ring degradation and side-chain degradation are carried out by many unidentified enzymes. The proposed pathway of cholesterol degradation in scheme 1-1 assumed that the side-chain degradation of cholesterol proceeds by a β-oxidation. C26 of cholesterol is assimilated into phthiocerol dimycocerosate (PDIM) that is an important virulence-associated lipid (*15*). However, the formation of androstenedione from the former carboxylate intermediate is not possible due to a secondary carbon of C17. This third round of the β-oxidation might actually proceed via α-oxidation.

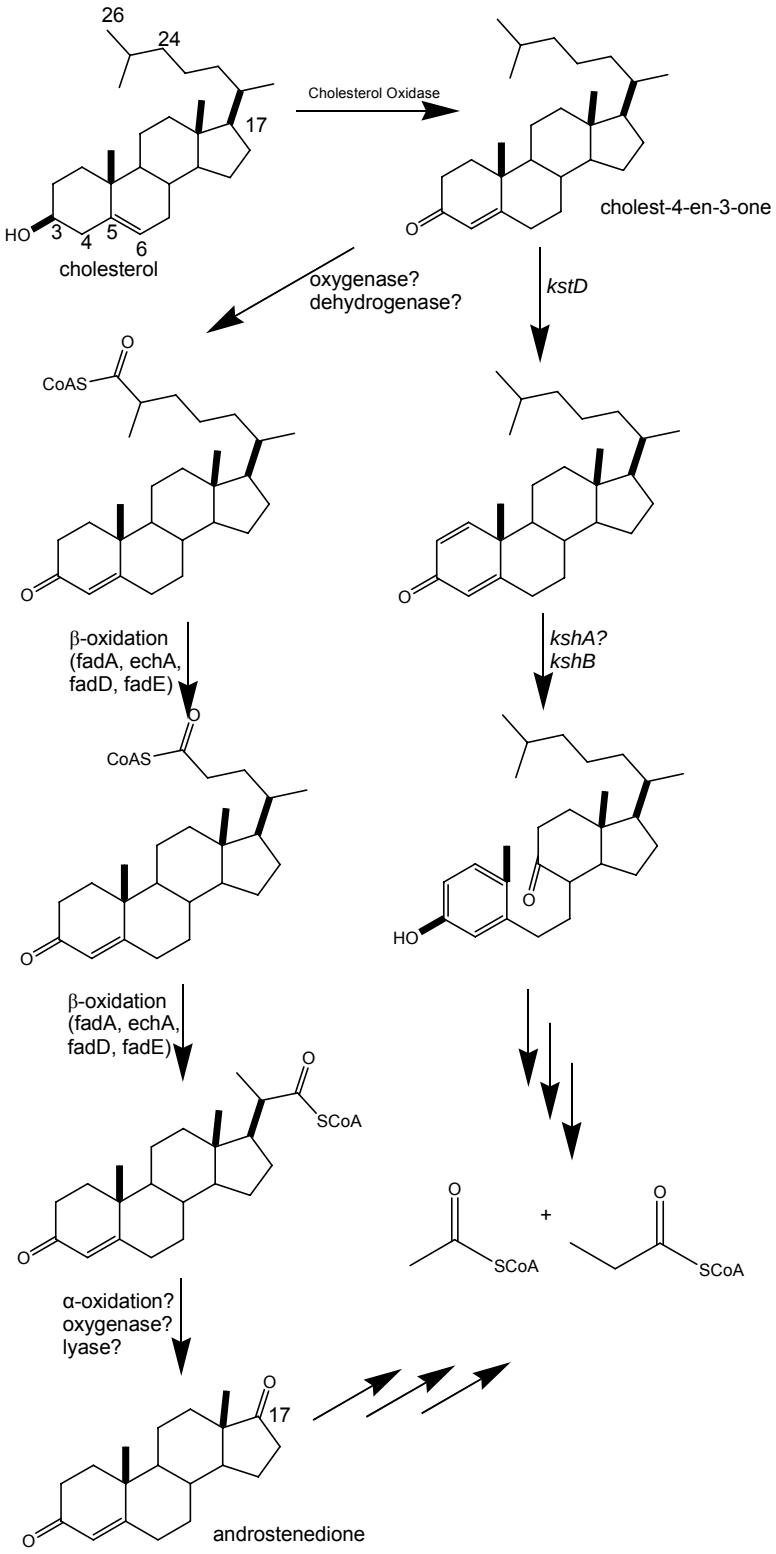

Scheme 1-1 A proposed pathway of bacterial cholesterol degradation based on the studies in *Rhodococcus* (*18*), Comamonas testosteroni (*19, 20*), and *M. smegmatis* (*21*).

The dehydrogenation is the next step of ring degradation, proceeding via the enzyme encoded by *kstD* or *ksdD* genes in *Rhodococcus* (*22, 23*) and *Mycobacterium smegmatis* (*M. smeg*) respectively (*24*). The disruption of the *kshA* gene in *Rhodococcus* did not inhibit the bacterial growth on sitosterol (24-ethyl cholesterol) while the growth on androstenedione was prevented (*18*). The disruption of the same gene in *M. smeg* converted sitosterol to androstenedione, but there was not further degradation (*21*). These studies elucidate that there are two pathways of sterol degradation in *Rhodococcus*, one pathway for the C27-C29 steroids and another one for the C19 steroids like androstenedione, and there is only one pathway in *M. smeg*.

There are some results about cholesterol metabolism in *M. tb* until now. *M. tb* can grow in the culture of soluble cholesterol, as a primary carbon source, and cholesterol degradation by *M. tb* can convert C4 to CO_2 and C26 to PDIM (*15*). C4 is cleaved as a pyruvate (*25*) unit and it is converted to CO_2 through the tricarboxylic acid cycle. Different from the 4 carbon, in other organisms C26 is cleaved as a propionyl-CoA unit (*26*) and it is incorporated into lipids including PDIM in *M. tb* (*27*). *hsaC* and *hsaD*, genes postulated to be required for cholesterol metabolism, were expressed in *E. coli* and these catalyzed the 3,4-DSHA (3,4-dihydroxy-9,10-seconandrost-1,2,3-triene-9,17-dione) to 4,9-DHSA and 4,9-DHSA to DOHNAA (9,17-dioxo-1,2,3,4,10,19-hexanorandrostan-5-oic acid), respectively (*28*). *cyp51* from *M. tb*, catalyzes sterol 14α-demethylation as a key step of sterol biosynthesis, was expressed in *E. coli*, but other genes involved in the sterol biosynthesis are missing in the genome of *M. tb* (*29*). In addition, it was found that *Rv1106c* encodes 3β-hydroxysteroid dehydrogenase (3β-HSD) (*30*) and *M. tb* requires this gene for growth on cholesterol as a sole carbon source.

By transcriptional profiling, it was discovered that there are 58 genes regulated by cholesterol in an 82-gene cluster in *Rhodococcus* RHA1 (*28*). The majority of these genes are conserved in *M. tb* and several of these genes are up-regulated during *M. tb* infection of macrophages and in mice (*31, 32*). In our lab, the transcriptional profile of *M. tb* genes induced by cholesterol was analyzed and the results compared to the results for the genes in *Rhodococcus* RHA1. Even though there are many similarities between *M. tb* genes and the genes of *Rhodococcus* RHA1, there are still many differences in the regulons. We postulate that there must be another pathway of cholesterol degradation in *M. tb*.

2. The disorder in a host membrane

Cholesterol is involved in the entry of *M. tb* into macrophages and the survival of *M. tb* there (*14*). Cholesterol oxidases perform the oxidation and isomerization of cholesterol to cholest-4-en-3-one in a lipid bilayer. The disorder in a host membrane increases by this reaction and lysis of the membrane or leakage of intracellular contents result (*33, 34*). *Rhodoccucos equi* (*R. equi*) is an actinomycete pathogen that metabolizes cholesterol. This pathogen also causes serious tissue damage like *M. tb*. The c*hoE* gene, encodes a cholesterol oxidase, in *R. equi*. The activity of ChoE is related to the haemolytic activity that is able to oxidize cholesterol in the macrophage membrane and grow in macrophages of mouse (*35*). Moreover, the c*hoE* knock-out from *R. equi* lost its membrane damaging ability (*36*) and *R. equi* infection was attenuated in 3-week old foals (*37*). These studies proposed that cholesterol oxidases are involved in maintaining intracellular infection.

3. Secondary metabolism of cholesterol

Glucocorticoids are immunosuppressive and anti-inflammatory agents (*38*) biosynthesized from cholesterol (scheme 1-2).

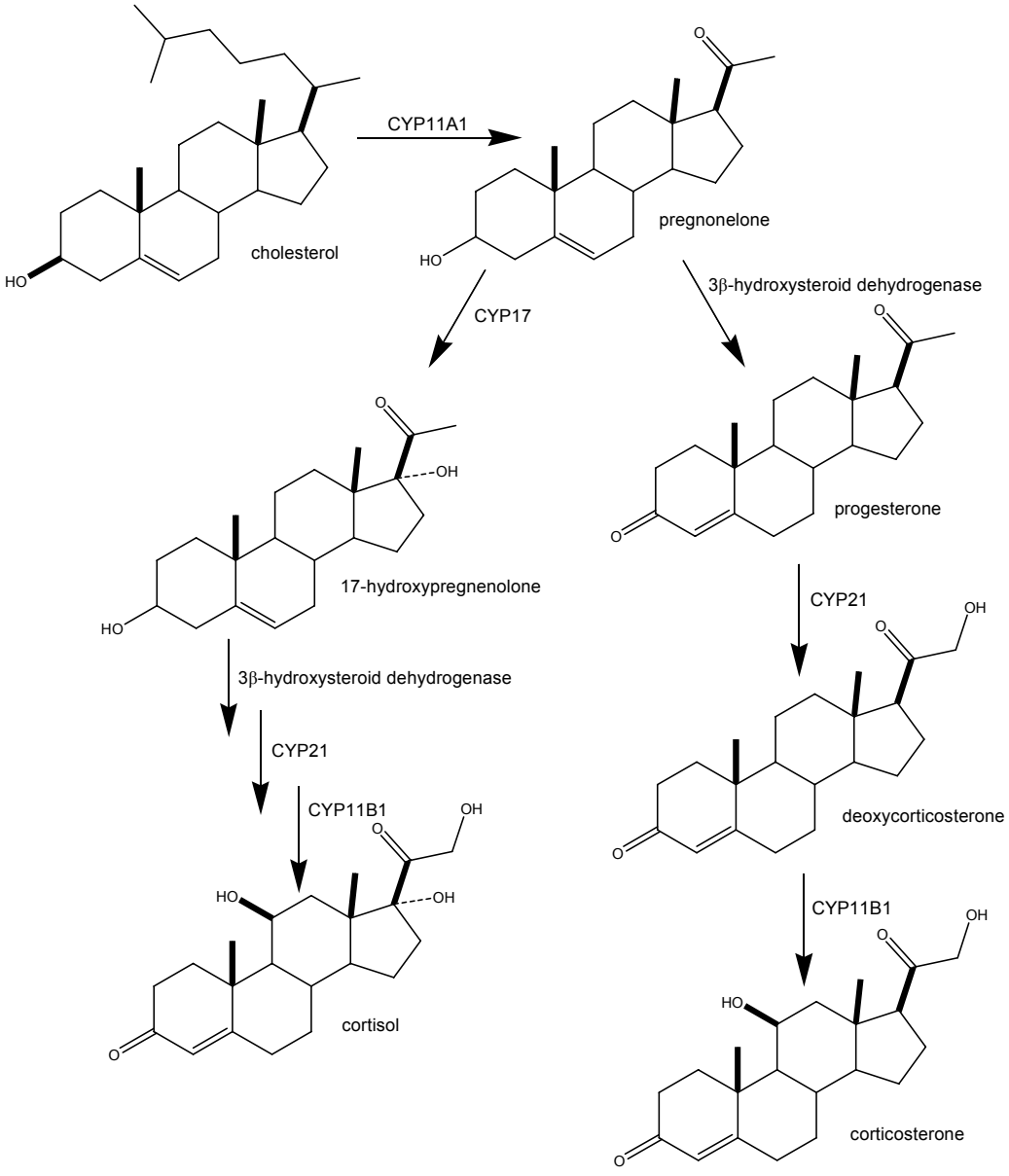

Scheme 1-2 Mammalian glucocorticoid biosynthesis

Progesterone is a precursor of corticosteroids that is converted from pregnenolone by 3β-HSD. Corticosteroids are involved in the immune system by blocking the production of the substrates that cause inflammatory and allergic actions. However, they disturb the function of white blood cells and weaken immune system function. In vaccinia virus, corticosteroids are produced in the infected host and this production requires *3β-hsd* gene. Deletion of the gene encoding for 3β-HSD attenuated the level of infectivity in the lungs and strengthened the activity of immune systems in infected mice (*39*). These studies showed that the activity of the 3β-HSD contributes to host immunosuppression to ensure robust infection. *Rv1106c* of *M. tb* encodes a 3β-HSD (*30*) and it is close to the *3β-hsd* gene of vaccinia virus in an evolutionary tree. Thus, it may have a similar function in *M. tb* infection.

Mammalian corticosteroids are not the only bioactive steroid structure found in nature. For example, brassinolides are biosynthesized from campesterol in plants (*40*) and ecdysone is synthesized from cholesterol in insects (*41*). Biosynthesis of these steroid hormones requires a 3β-HSD and cytochrome P450 enzymes. The *M. tb* genome includes 20 cytochrome P450 enzymes and this high density of cytochrome P450 genes suggests that the mono-oxygenase chemistry of cytochrome P450 enzymes might be heavily involved in the metabolism including cholesterol to produce sterol hormones.

4. Detoxification by cholesterol degradation

M. tb is exposed to host membranes when it resides in granulomas and the detoxification mechanism of host membranes might be required. The host membranes contain cholesterol and the products of cholesterol degradation may be involved in primary or secondary metabolism.

CHAPTER 2

Characterization of Rv3545c, Putative CYP125, from *Mycobacterium tuberculosis*

I. Introduction

II. Materials and methods

III. Results and discussion

I. Introduction

The sequence of the *M. tb* genome was determined about 10 years ago revealing that there are several ORFs predicted to encode enzymes correlated with cholesterol metabolism in the genome (*1*).

There are several postulations about the function of cholesterol degradation. One of the postulations is the secondary metabolism of cholesterol to sterol hormones. Mammals are able to biosynthesize cholesterol to glucocorticoids, immunosuppressive and anti-inflammatory agents (*2*). Corticosteroids are synthesized from cholesterol. 3β-hydroxysteroid dehydrogenase converts pregnenolone to pregesterone which is synthesized to corticosteroids by many other cytochrome P450 enzymes. Corticosteroids are usually correlated with the immune system, weakening its function by disturbing the white blood cell role. In vaccinia virus, which is the small pox vaccine, corticosteroids are produced in the infected host and the deletion of the gene encoding a 3β-HSD attenuated the level of infectivity in the lungs, strengthening the activity of the immune system in infected mice (*3*). 3β-HSD is encoded by *Rv1106c* gene in *M. tb* (*4*) and twenty different cytochrome P450 enzymes are encoded in the *M. tb* genome (*1*). These facts suggest that the function of cholesterol degradation in *M. tb* may be the synthesis of corticosteroids that may regulate the host immune response.

The cytochrome P450 enzyme is a heme-containing enzyme. The name "cytochrome P450" comes from the fact that it has an absorbance peak at 450 nm when its Fe(II) state reacts with carbon monoxide. The P450 catalyzes the mono-oxygenation of a lot of substrates. The substrate (R-H) binds to Fe(III) (ferric state) of cytochrome P450 and Fe(III) is reduced to Fe(II) (ferrous state) by a single electron (e^-). Then

dioxygen binds to the iron to make the ferrous to ferric again. Addition of another electron and two protons forms the transient state intermediate that is converted to the mono-oxygenated substrate and produces a water molecule (*5*). In this step, two electrons are from NAD(P)H by redox partner(s) and two protons are usually from bulk solvent by active site amino acid side chains (*6*). The heme finally returns to the ferric state by the dissociation of the product.

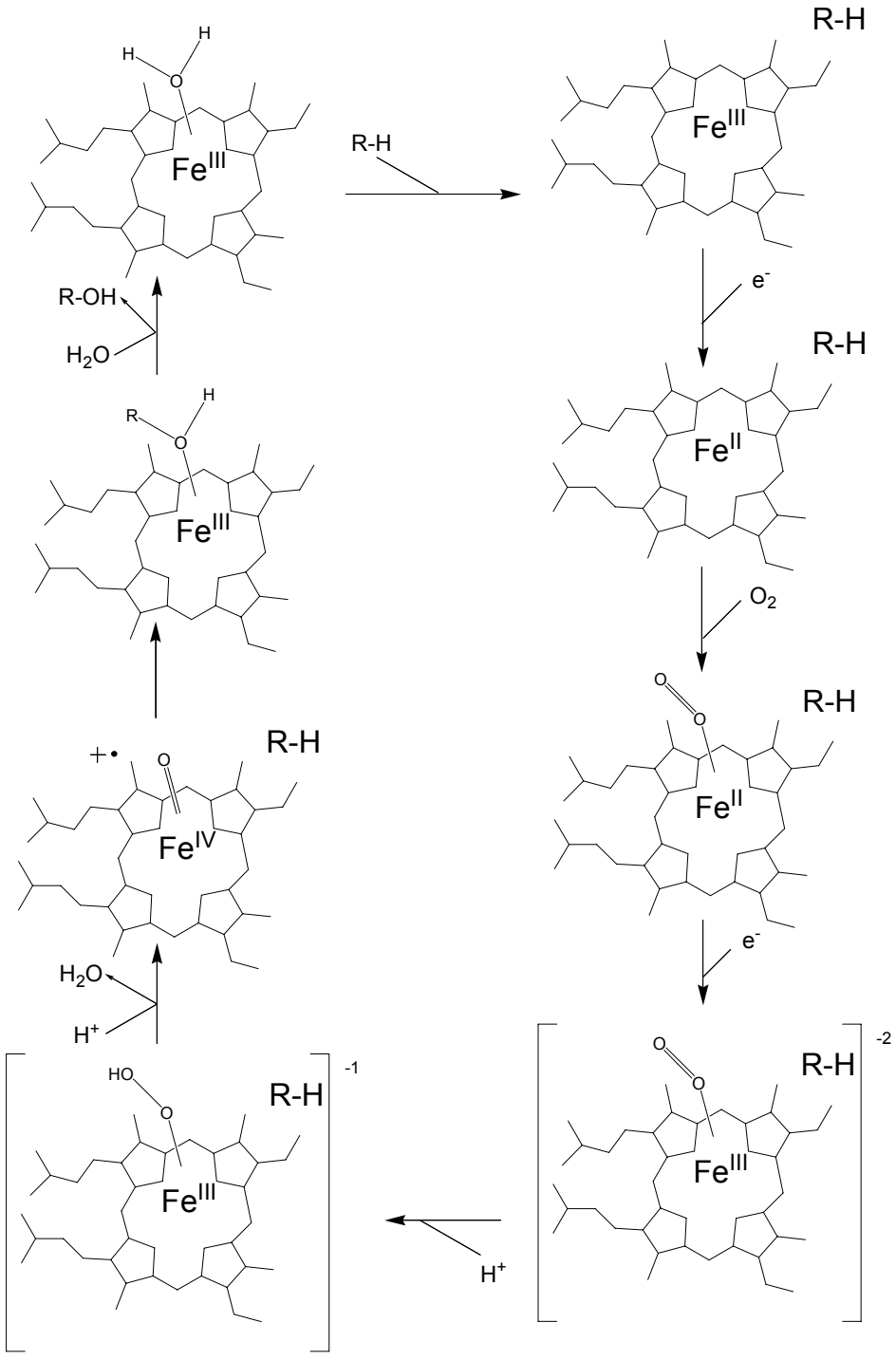

Scheme 2-1 Catalytic cycle of cytochrome P450

P450 enzymes are present in many living organisms including bacteria and mammals. To exemplify, *S. coelicolor* has 18 genes encoding P450 enzymes (*7*) and *M. bovis* has 18 *cyp* genes (*8*). An interesting fact is that the size of *Escherichia coli* (*E.coli*) genome is similar and it is completely devoid of P450 genes (*9*) while *M. tb* has twenty genes encoding P450 enzymes. In addition, the human genome whose size is 600 times greater than *M. tb*'s encodes only 57 P450 enzymes (*10*). This high density of cytochrome P450 genes suggests that mono-oxygenase chemistry of cytochrome P450 enzymes might be heavily involved in *M. tb* virulence.

Until now, only three *M. tb* P450 enzymes have been characterized structurally. One of the enzymes is CYP51 (encoded by *Rv0764c*), a bacterial sterol 14α-demethylase (*11, 12*). The determination of *M. tb* CYP51's atomic structure, in complex with fluconazole (azole inhibitor), gave the first insight into the 3-dimensional architecture of a sterol demethylase P450 (*13*). There is a substantial distortion of the I helix region of the enzyme and it contains important residues for substrate recognition and orientation, and for catalysis of oxygenation chemistry (*14, 15*). The early studies on CYP51 indicated that it is able to catalyze 14α-demethylation of lanosterol, 24, 25-dihydrolanosterol and the plant sterol obtusifoliol, then produce 8,14-diene products (*16*). Furthermore, the CYP51 has azole and triazole binding affinity so it is known as a target for azole and triazole drugs (*e.g.* fluconazole, clotrimazole, miconazole etc) in fungi and yeast (*17*).

Another structurally characterized *M. tb* P450 enzyme is CYP121 encoded by *Rv2276* (*18*). Even though it does not have the similar amino acid sequence with other P450 enzymes in the databases, the purified enzyme has tight binding with a range of

azole antifungal drugs. Moreover, the crystal structure of CYP121 revealed the conformation of the enzyme and the aspects of heme binding (*19*).

CYP130 is encoded by *Rv1256c* in *M. tb* (*20*). It also has binding affinity to azole drugs. X-ray crystallography experiments revealed that this enzyme has two conformers. The inhibitor is enveloped in the binding site by the conformational change of the BC-loop and the F and G helices and the protein surface is reshaped. When CYP130 is crystallized without ligand, it is a monomer in an open conformation. A dimer in a closed conformation is formed as the econazole was bound to CYP130.

Beside CYP51, CYP121, and CYP130, there are many other P450 enzymes from *M. tb* H37Rv (Table 2-1). Among them, CYP125 is especially highlighted in this chapter. The operon, *Rv3540c-Rv3545c*, contains *cyp125*, and is up-regulated in macrophages and required for survival in macrophages (*21, 22*). Chang, J.C. *et al*. named the operon as *igr* region (intracellular growth restriction region) and identified that this region is important for intracellular survival, but not required for fatty acid utilization (*23*). However, microarray analysis and qrt-PCR data, done by our lab, revealed that the genes in *igr* region are up-regulated and induced by cholesterol and macrophages in *M. tb*. To identify the correlation between cholesterol metabolism and *igr* region in *M. tb*, further investigation is needed.

(a)

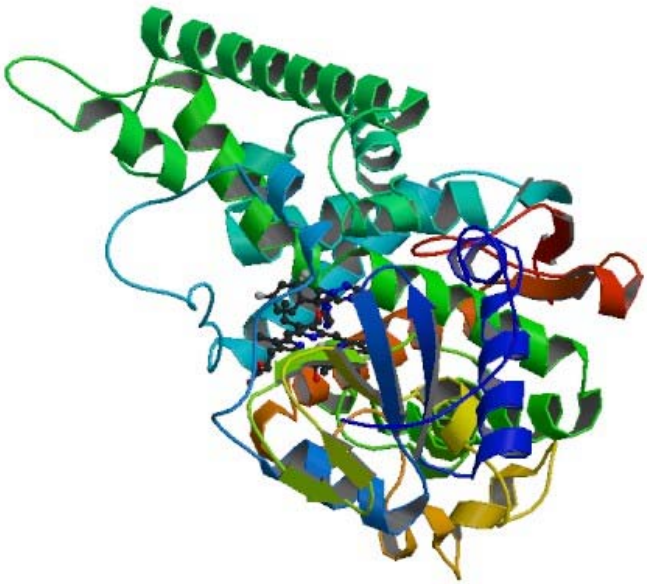

(b)

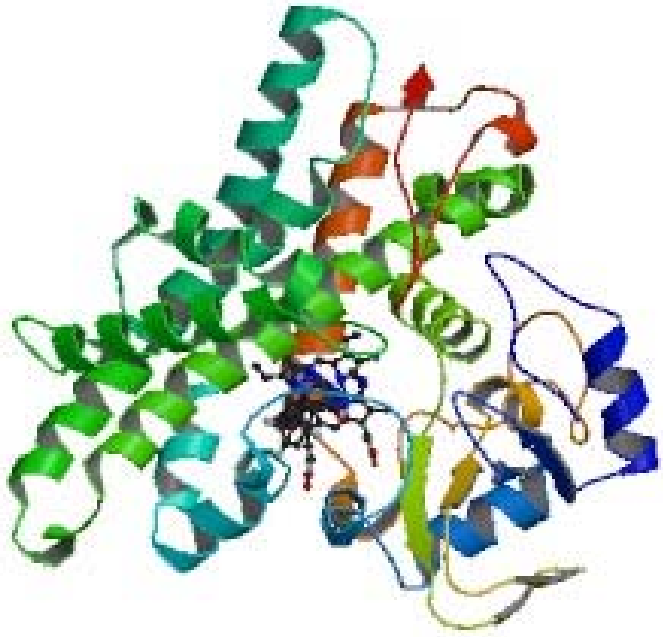

(c)

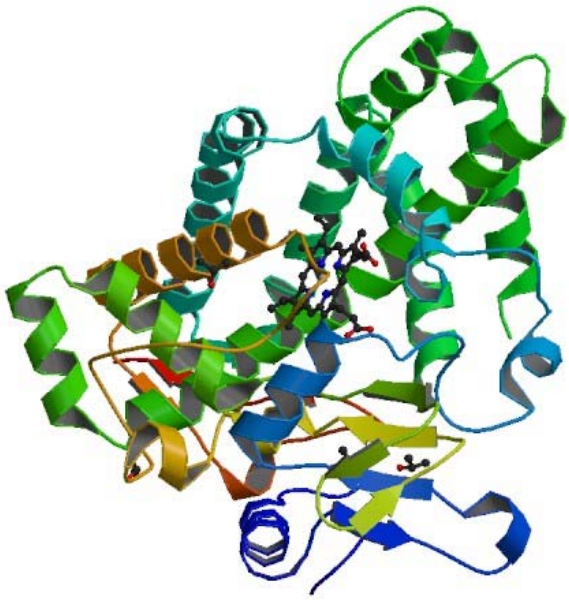

(d)

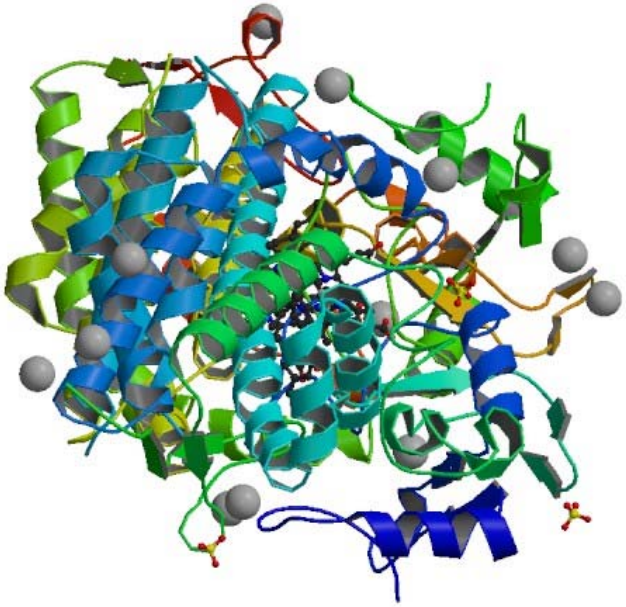

Figure 2-1 Atomic structures of (a) fluconazole-bound *M. tb* CYP51 (*12*), (b) fluconazole-bound *M. tb* CYP121 (*24*), (c) ligand-free *M. tb* CYP130 (*20*), and (d) econazole-bound *M. tb* CYP130 (*20*)

Protein name	*M. tb* gene	Microarray/genetic analysis	Key facts
CYP51	*Rv0764c*	Non-essential gene. Role in host sterol/steroid inactivation (*25*)?	Sterol 14α-demethylase. Structures solved for ligand-free and for substrate analogue- and fluconazole-bound forms (*12*)
CYP121	*Rv2276*	Putative essential gene. Possible role in virulence through studies with ΔAraC/XylS gene regulator mutant (Δ*Rv1931c*). induced in isoniazid- and thiolactomycin-treated *M. tb*	Nanomolar azole drug affinity. Highest resolution P450 structure (*19*). Novel azole binding mode (*24*)
CYP123 & CYP138	*Rv0766c* & *Rv0136*	Upregulated at high temperatures (*26*)	CYP123 may form operon with CYP51 and its adjacent ferredoxin Fdx
CYP125	*Rv3545c*	Induced in macrophages. Essential for infection in mice (*27*)	Tight azole drug binding. Adjacent to genes involved in lipid degradation
CYP128	*Rv2268c*	Possible essential gene. Required for *M. tb* growth *in vitro* (*28*). Expression upregulated post-starvation	*CYP128* adjacent to lipoprotein genes. Function may be related to those of P450s encoded by nearby *CYP121* and *CYP124*
CYP130	*Rv1265c*	Absent from *M. bovis* BCG vaccine strain (deletion RD13)	Adjacent to oxidoreductase
CYP132	*Rv1394c*	Possible role in *M. tb* virulence. Transcription controlled by adjacent AraC transcriptional regulator (*29*)	Similar to fatty acid metabolizing P450s
CYP141	*Rv3121*	Absent from *M. bovis* BCG vaccine strain (deletion RD13)	Surrounding genes involved in molybdenum cofactor biosynthesis
CYP144	*Rv1777*	Possible role in virulence	Tight azole drug binding. Adjacent to genes likely involved in membrane metabolism

Table 2-1 Key facts about P450 enzymes from *Mycobacterium tuberculosis* H37Rv (*30*)

II. Materials and methods

Materials

δ-aminolevulinic acid was purchased from MP Biomedicals, LLC (Solon, Ohio). TALON Metal Affinity Resin was from Clontech Laboratories, Inc. (Mountain View, CA) *Pfu* DNA polymerase was from Stratagene (La Jolla, CA), and restriction endonucleases, calf intestinal alkaline phosphatase (CIP), and T4 DNA ligase were purchased from New England Biolabs (Beverly, MA). Isopropyl-β-D-thiogalactopyranoside (IPTG) was from Anatrace (Maumee, Ohio), and phenylmethanesulphonylfluoride (PMSF) was from ALEXIS Biochemicals (San Diego, CA). All other chemical reagents were purchased from Fisher Scientific (Pittsburg, PA). Water used for assays and chromatography was distilled by Barnstead NANOpure ultrafilter system.

Buffers and Media

Luria broth (LB) medium: 20 g LB in 1 L DDI H_2O; 0.1 M K-Pi buffer: 13.968 g K_2HPO_4, 2.696 g KH_2PO_4 in 1 L DDI H_2O; Trace elements solution: 1.765 g/L EDTA, 10.95 g/L $ZnSO_4 \cdot 7H_2O$, 5 g/L $FeSO_4 \cdot 7H_2O$, 1.54 g/L $MnSO_4 \cdot H_2O$, 0.392 g/L $CaSO_4 \cdot 5H_2O$, 0.248 g/L $Co(NO_3)_2 \cdot 6H_2O$, 0.114 g/L H_3BO_3; 7H9 protein expression medium: 4.7 g 7H9 middlebrook broth, 0.2% (v/v) glycelrol, 0.2% (w/v) glucose, 0.05% (v/v) Tween-80 in 1 L DDI H_2O; 7H9 rich medium: 4.7 g 7H9 middlebrook broth, 0.2% (v/v) glycerol, 1XADS, 0.05% (v/v) Tween-80 in 1 L DDI H_2O; 10XADS: 8% NaCl, 10% BSA fraction V, 4% glucose in 1 L DDI H_2O; 1 M Tris-HCl: 121.14 g Tris, ~65 mL HCl (to adjust pH to 7.2) in 1 L DDI H_2O; Buffer A: 50 mM Tris-HCl + 1 mM EDTA;

Buffer B: Buffer A + 300 mM NaCl; Buffer C: Buffer A + 300 mM NaCl + 8 M Urea; Buffer D: Buffer A + 300 mM NaCl + 150 mM imidazole

Methods

General method of plasmid construction for CYP125

The plasmid containing the gene of interest was amplified by the polymerase chain reaction (PCR). The two primers were designed as follows: YG01: 5' – GCCGCCGCCCAT**ATG**TCGTGGAATCACCAG – 3'. This primer is a 30-base oligonucleotide that encodes the first five codons of *Rv3545c* gene. The bold letters show the initiation codon ATG, and the underlined letters indicate the restriction site for *Nde* I. YG02-r: 5' – GGCGGCGGCAAGCTTGTGAGCAACCGGGCA – 3'. This second primer is also a 30-base oligonucleotide and encodes the reverse complement of the last five codons of *Rv3545c*. The underlined letters indicate the restriction site for *Hind* III. The mixture for PCR was prepared with 400 ng plasmid, 400 μM each dNTP, 0.25 μM of each primer, 2.5 U *Pfu* DNA polymerase, and 2.75 mM Mg^{2+} in *Pfu* buffer. The mixture was heated at 98 °C for 1 min and cycled 30 times with a cycle of 98 °C (45 sec), 73 °C (1 min), and 72 °C (3 min). The mixture was heated at 72 °C for an addition 10 min and then stored at 4 °C. The vector was double digested with 20 U *Nde* I, 20 U *Hind* III, and 10 U CIP in NEBuffer 2 at 37 °C for 1.5 h. The PCR fragments were double digested the same way without CIP. The ligation of the vector and the PCR fragments was carried out with T4 ligase in T4 ligase buffer at 16 °C overnight. The ligation mixture was transformed into XL1Blue competent cells and the plasmid was purified by Wizard Plus SV minipreps (Promega). The identification of the insert in the purified plasmid was carried out by double digestion with *Nde* I and *Hind* III restriction enzymes. The DNA

sequences of the plasmids were verified with T7-promoter (PC-05: 5' – TAATACGACTCACTATAGGG – 3') and the 571-600 sequence of *Rv3545c* gene (NN63: 5' – GGCAAGCTGTTCCACTGGTCAAACGAGATG – 3') from the Stony Brook University DNA sequencing Facility.

The plasmid containing N-terminal his-tagged *cyp125* (in pET28a vector) was a gift from Astra Zeneca. The plasmid for C-terminal his-tagged CYP125 was constructed by inserting the gene of *Rv3545c* into pET20b vector. *Rv3545c* was inserted into pET28b vector to construct the plasmid containing N and C-terminal his-tagged *cyp125*. *cyp125* gene was inserted into pVV16 shuttle vector to grow the protein in *M. smegmatis*. This construct let the protein have C-terminal his-tag. When constructing the new plasmids, the stop codon (TAA) located at the end of the gene sequence was mutated to AAG.

Expression of CYP125 in *Escherichia coli*

The plasmid was transformed into *Escherichia coli* (*E. coli*) strain competent cell, and colonies were grown on a LB-agar plate containing appropriate antibiotic. The plate was placed at 37 °C overnight. A single colony was inoculated in a 10 mL LB culture, containing proper antibiotic, in a sterilized transformation tube at 37 °C and 250 RPM overnight. 1 mL of the inoculated culture was taken to inoculate 50 mL of LB medium containing 0.1 M K-Pi buffer and 0.4% glycerol, and it was grown at 37 °C until the $O.D._{600}$ = 0.6. The temperature was lowered to 18 °C and the culture was allowed to equilibrate. 1 mM δ-aminolevulinic acid was added and the culture was induced by 0.2 mM IPTG for 20 h. The cells were harvested by centrifugation at 4,000 X *g* for 20 min (4 °C). The cells were washed by resuspension in Buffer B and harvested again. The pellet was stored at -20°C until use.

Three plasmids, containing N-terminal, C-terminal and N and C-terminal his-tagged *cyp125* genes, were transformed into BL21(DE3)pLysS competent cell and those plasmids were also transformed into Rosetta(DE3) and Rosetta2(DE3) competent cells. 200 μg/mL ampicillin was used as an antibiotic for N-terminal and N and C-terminal his-tagged CYP125 and 50 μg/mL kanamycin was for C-terminal his-tagged protein.

Expression of CYP125 in *M. smegmatis*

The plasmid constructed with the insertion of *Rv3545c* gene in pVV16 vector was transformed into *M. smegmatis* competent cell and colonies were grown on a LB-agar plate containing 100 μg/mL hygromycin B. The plate was placed at 37 °C for 4 days. A single colony was inoculated in 3 mL of 7H9 rich medium containing 100 μg/mL hygromycin B, in a sterilized transformation tube at 37 °C and 250 RPM overnight. The inoculated culture was taken to inoculate a 100 mL 7H9 protein expression medium, and it was grown until an $O.D._{600}$ = 0.6 at 35.5 °C. 1 mM δ-aminolevulinic acid was added and the culture was induced by 0.01% acetamide for 20 h. The cells were harvested by centrifugation at 4,000 X *g* for 20 min (4 °C). The cells were washed with Buffer B. the pellets was harvested again and stored at -20°C.

Purification of CYP125 by metal affinity resin

The cells were thawed and resuspended in a small amount of Buffer B containing 1 mM PMSF. The cells were lysed by sonication (Fisher Scientific, for *E. coli* six times for 5 sec bursts at power 6 on ice with 30 sec cooling between bursts, and for *M. smeg* six times for 40 sec bursts at power 6 on ice with 1 min resting). The cell extracts were centrifuged at 10,000 X *g* for 20 min (4 °C) and the supernatant was separated from the pellet. 8 M urea was added to half of the supernatant to denature the soluble proteins. The

pellet was resuspended in Buffer C. TALON Metal Affinity resin for native supernatant was pre-equilibrated in Buffer B and the resins for denatured supernatant and pellet were pre-equilibrated in Buffer C. The polyhistidine-tagged proteins resuspended in supernatant and pellet were allowed to bind to the TALON resins. The resins were washed with the appropriate buffers and the bound proteins were eluted by Buffer D.

Assessment of CYP125

The process of constructing the plasmids was observed by 1% agarose DNA gels. The expression of CYP125 was determined by 12% SDS-PAGE gel electrophoresis.

III. Results and discussion

There are three *M. tb* P450 proteins that have been structurally identified: CYP51, CYP121, and CYP130 (*11, 18, 20*). Each of these proteins were expressed and purified in different conditions. CYP51 had a C-terminal his-tag and it was transformed into HMS174(DE3). CYP121 was expressed without polyhistidine tags and was transformed into HMS174(DE3). Moreover, N-terminal his-tagged CYP130 was expressed in DH5α(DE3) competent cells. Even though those are all P450 proteins, each protein requires different conditions from others. To express CYP125 successfully, different location of his-tags in protein and several kinds of competent cells were tested.

The plasmid containing N-terminal his-tagged *cyp125* was a gift from Astra Zeneca and it was constructed by inserting the *cyp125* gene sequence between *Nde* I and *Hind* III restriction sites into pET28a vector. The plasmid was transformed into BL21(DE3)pLysS competent cells and expressed according to the procedure of Podust and co-works (*31*). One difference was that several media conditions were used to find one suitable for cyp125 expression (Table 2-1).

Culture #	Components of the culture	δ-aminolevulinic acid (1mM)
1	LB	X
2	LB	O
3	LB, 0.1 M K-Pi buffer, 0.4% glycerol, 50 mg/L ferric ammonium citrate	O
4	LB, 0.1 M K-Pi buffer, 0.4% glycerol, 0.10 ml trace elements solution	O
5	LB, 0.1 M K-Pi buffer, 0.4% glycerol	O

Table 2-2 The components of the cultures and the addition of δ-aminolevulinic acid

McLean and co-workers successfully expressed and purified CYP121 (*18*). When the cells were induced at high temperature (37 ºC), the cells did not express soluble CYP121 on lysis of transformant cells and the protein did not incorporate heme (*32*). In addition, δ-aminolevulinic acid was required as a precursor of heme biosynthesis during CYP51 induction, while it was not necessary for CYP121 expression (*18, 31*). So, those cultures were induced at low temperature, 18 ºC, with low concentration of IPTG (0.2 mM). δ-aminolevulinic acid was also added to cultures 2-4 only (Table 2-1). After sonication and centrifugation, the TALON Metal Affinity experiment was carried out for those four different cultures. SDS-PAGE was utilized to determine whether CYP125 (MW 48 kDa) was expressed or not (Figure 2-2).

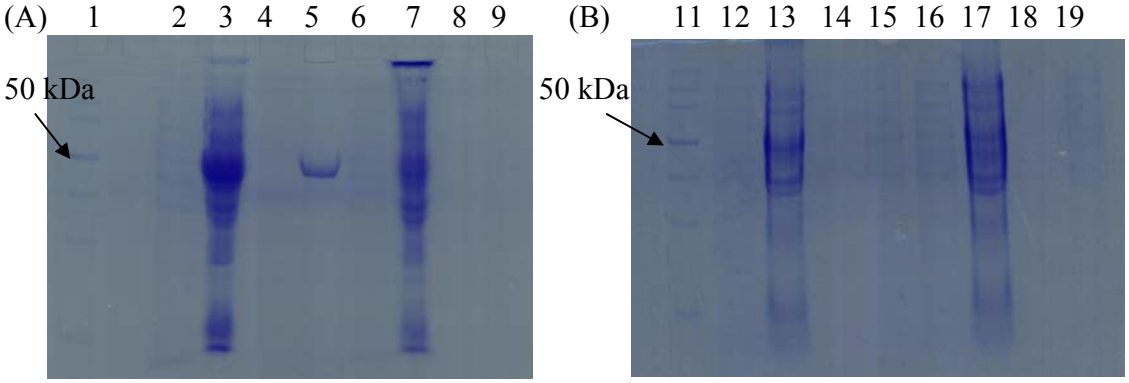

Figure 2-2 SDS-PAGE of N-terminal his-tagged CYP125 expressed in BL21(DE3) from cultures 1-4

(A) Lane 1: Protein Marker; for culture 1, Lane 2: supernatant before TALON Metal Affinity experiment (TALON), Lane 3: pellet before TALON, Lane 4: supernatant after TALON, Lane 5: pellet after TALON; for culture 2, Lane 6: supernatant before TALON, Lane 7: pellet before TALON, Lane 8: supernatant after TALON, Lane 9: pellet after TALON

(B) Lane 11: Protein Marker; for culture 3, Lane 12: supernatant before TALON, Lane 13: pellet before TALON, Lane 14: supernatant after TALON, Lane 15: pellet after TALON; for culture 4, Lane 16: supernatant before TALON, Lane 17: pellet before TALON, Lane 18: supernatant after TALON, Lane 19: pellet after TALON

For culture 2-4, no CYP125s were expressed and attached to TALON Metal Affinity Resin. From culture 1 a lot of protein with the same MW as CYP125 was expressed, but all of them were insoluble even though expression conditions were at a low temperature and low concentration of IPTG. The insoluble proteins were attached to the TALON resin but do not have heme due to the denatured condition. As 8 M urea was added to the buffer the protein was unfolded and the bound heme was washed away. Even though the protein is refolded, it may not contain heme and it is not an active P450 enzyme anymore.

This time, the location of His-tag was changed from N-terminus to C-terminus. The plasmid containing C-terminal polyhistidine-tagged *cyp125* gene was constructed in the pET20b vector. The stop codon TAA, located at the end of *Rv3545c* gene, was mutated to *Hin*d III restriction sequence by PCR. This plasmid was transformed into BL21(DE3)pLysS competent cells and the cells were grown in culture conditions 1, 2, and 5. From all cultures, the proteins overexpressed but were all in inclusion bodies (Figure 2-3).

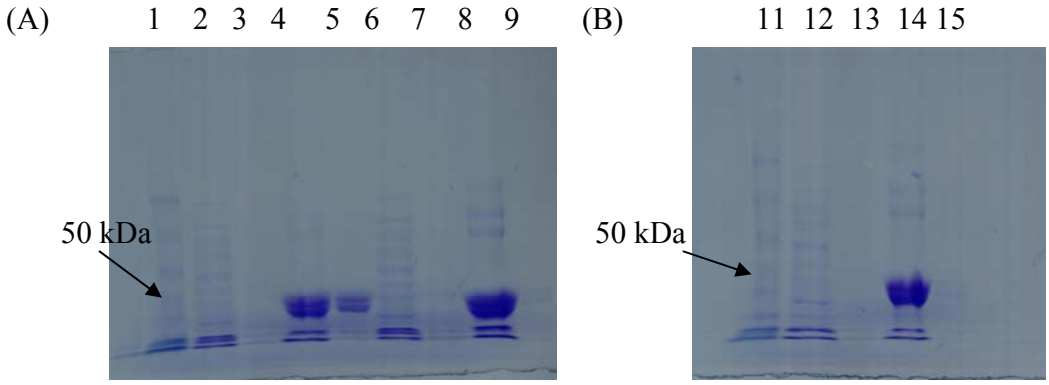

Figure 2-3 SDS-PAGE of C-terminal his-tagged CYP125 expressed in BL21(DE3) from cultures 1,2, and 5

(A) Lane 1: Protein Marker; for culture 1, Lane 2: supernatant before TALON Metal Affinity experiment (TALON), Lane 3: supernatant after TALON, Lane 4: pellet before TALON, Lane 5: pellet after TALON; for culture 2, Lane 6: supernatant before TALON, Lane 7: supernatant after TALON, Lane 8: pellet before TALON, Lane 9: pellet after TALON

(B) Lane 11: Protein Marker; for culture 5, Lane 12: supernatant before TALON, Lane 13: supernatant after TALON, Lane 14: pellet before TALON, Lane 15: pellet after TALON

Both N-terminal his-tagged CYP125 and C-terminal his-tagged CYP125 were expressed as insoluble proteins in BL21(DE3) competent cells, so Rosetta2(DE3) competent cells were used for expression. This competent cell is derived from BL21 and constructed to enhance protein expression which contain rarely used codons in *E. coli*. Two different plasmids, expressing N-terminal his-tagged CYP125 and C-terminal his-tagged CYP125, were transformed into BL21(DE3)pLysS and Rosetta2(DE3) competent cells and the cells were grew in culture 5. SDS-PAGE was carried out (Figure 2-4).

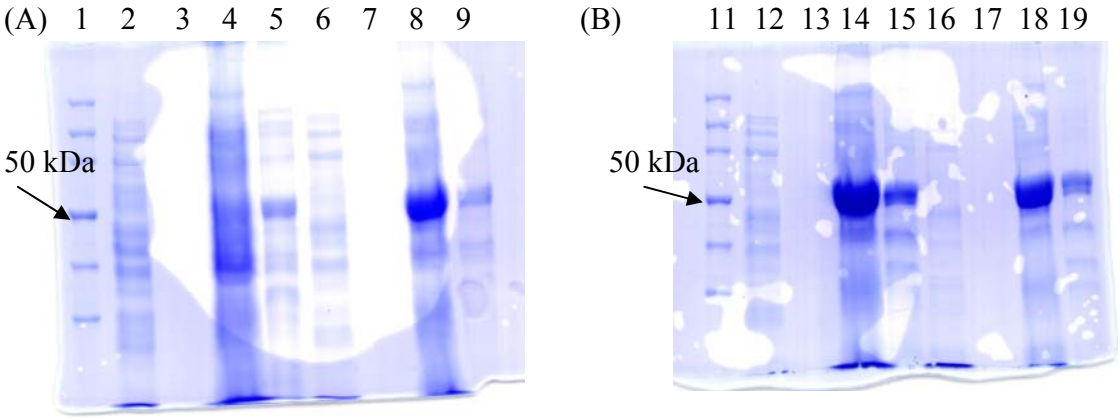

Figure 2-4 SDS-PAGE of N-terminal his-tagged CYP125 and C-terminal his-tagged CYP125 expressed in BL21(DE3) and Rosetta2(DE3)

(A) Lane 1: Protein Marker; for N-terminal his-tagged CYP125 expressed in BL21(DE3), Lane 2: supernatant before TALON Metal Affinity experiment (TALON), Lane 3: supernatant after TALON, Lane 4: pellet before TALON, Lane 5: pellet after TALON; for N-terminal his-tagged CYP125 expressed in Rosetta2(DE3), Lane 6: supernatant before TALON, Lane 7: supernatant after TALON, Lane 8: pellet before TALON, Lane 9: pellet after TALON

(B) Lane 11: Protein Marker; for C-terminal his-tagged CYP125 expressed in BL21(DE3), Lane 12: supernatant before TALON, Lane 3: 1supernatant after TALON, Lane 14: pellet before TALON, Lane 15: pellet after TALON; for C-terminal his-tagged CYP125 expressed in Rosetta2(DE3), Lane 16: supernatant before TALON, Lane 17: supernatant after TALON, Lane 18: pellet before TALON, Lane 19: pellet after TALON

For N-terminal his-tagged CYP125 it was not expressed as soluble or insoluble protein from BL21(DE3) but insoluble CYP125 was expressed in Rosetta2(DE3). For C-terminal his-tagged CYP125, from both BL21(DE3) and Rosetta2(DE3), only insoluble protein was expressed. Soluble protein could be obtained from both competent cells stains.

Vector pET28b was used to generate the construct allowing for expression of cyp125 with N and C-terminal his-tag. Three plasmids with N-terminal, C-terminal, and N and C-terminal his-tagged *cyp125* genes were transformed into three different competent cells, BL21(DE3)pLysS, Rosetta(DE3), and Rosetta2(DE3) competent cells. Rosetta(DE3) and Rosetta2(DE3) commonly supply six rare codons: AUA, AGG, AGA, CUA, CCC, and GGA. The only difference between those two competent cells is that

Rosetta2(DE3) supply one more rare codon, CGG, than Rosetta(DE3). The transformed cells were grown in culture 5. When TALON metal affinity experiment was carried out, the supernatant was divided into two and 8 M urea was added to one of them to denature the soluble protein. If denatured soluble protein binds to TALON resin, then the protein should be purified by other methods. The TALON resin was not washed this time to make sure that the bound proteins were not detached from the resin by washing. However, other bands, proteins not attached to the resin, were still remained due to not washing the resin when SDS-PAGE was carried out. Consequently, the results of TALON metal affinity experiment were not clear; many bands appeared on the gel (Figure 2-5). In BL21(DE3), only C-terminal his-tagged CYP125 was expressed, but it was insoluble. In Rosetta(DE3) and Rosetta2(DE3), N-terminal, C-terminal, and N and C-terminal his-tagged proteins were all expressed but the majority was present in inclusion bodies. However, a small amount of soluble N-terminal and N and C terminal his-tagged proteins seemed to be expressed in Rosetta(DE3) and Rosetta2(DE3), respectively (red circles from Figure 2-5 (C) and (F)). If those are the target proteins, the soluble CYP125 is able to be purified from a large amount of culture.

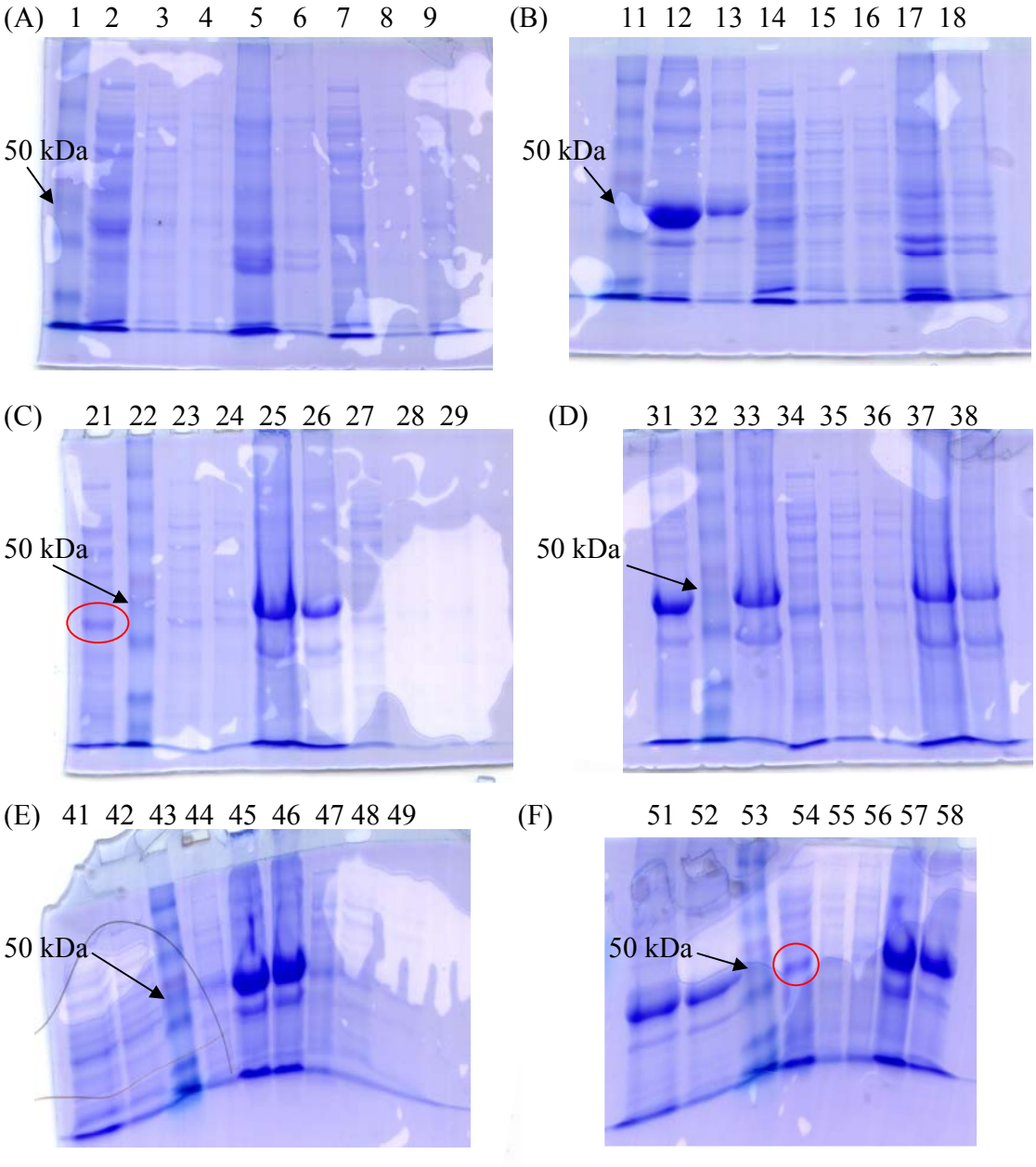

Figure 2-5 SDS-PAGE of N-terminal, C-terminal, and N and C-terminal his-tagged CYP125s expressed in BL21(DE3), Rosetta(DE3), and Rosetta2(DE3)

(A) **In BL21(DE3)** Lane 1: Protein Marker; for N-terminal his-tagged CYP125, Lane 2: supernatant before TALON Metal Affinity experiment (TALON), Lane 3: supernatant after TALON, Lane 4: denatured supernatant after TALON, Lane 5: pellet before TALON, Lane 6: pellet after TALON; for C-terminal his-tagged CYP125, Lane 7: supernatant before TALON, Lane 8: supernatant after TALON, Lane 9: denatured supernatant after TALON

(B) **In BL21(DE3)** Lane 11: Protein Marker; for C-terminal his-tagged CYP125, Lane 12: pellet before TALON, Lane 13: pellet after TALON; for N and C-terminal his-tagged CYP125, Lane 14: supernatant before TALON, Lane 15: supernatant after TALON, Lane 16: denatured supernatant after TALON, Lane 17: pellet before TALON, Lane 18: pellet after TALON

(C) **In Rosetta(DE3)** Lane 22: Protein Marker; for N-terminal his-tagged CYP125, Lane 21: supernatant before TALON Metal Affinity experiment (TALON), Lane 23: supernatant after TALON, Lane 24: denatured supernatant after TALON, Lane 25: pellet before TALON, Lane 26: pellet after TALON; for C-terminal his-tagged CYP125, Lane 27: supernatant before TALON, Lane 28: supernatant after TALON, Lane 29: denatured supernatant after TALON

(D) **In Rosetta(DE3)** Lane 32: Protein Marker; for C-terminal his-tagged CYP125, Lane 31: pellet before TALON, Lane 33: pellet after TALON; for N and C-terminal his-tagged CYP125, Lane 34: supernatant before TALON, Lane 35: supernatant after TALON, Lane 36: denatured supernatant after TALON, Lane 37: pellet before TALON, Lane 38: pellet after TALON

(E) **In Rosetta2(DE3)** Lane 43: Protein Marker; for N-terminal his-tagged CYP125, Lane 41: supernatant before TALON Metal Affinity experiment (TALON), Lane 42: supernatant after TALON, Lane 44: denatured supernatant after TALON, Lane 45: pellet before TALON, Lane 46: pellet after TALON; for C-terminal his-tagged CYP125, Lane 47: supernatant before TALON, Lane 48: supernatant after TALON, Lane 49: denatured supernatant after TALON

(F) **In Rosetta2(DE3)** Lane 53: Protein Marker; for C-terminal his-tagged CYP125, Lane 51: pellet before TALON, Lane 52: pellet after TALON; for N and C-terminal his-tagged CYP125, Lane 54: supernatant before TALON, Lane 55: supernatant after TALON, Lane 56: denatured supernatant after TALON, Lane 57: pellet before TALON, Lane 58: pellet after TALON

To purify the soluble proteins by TALON metal affinity experiment, fresh colonies, Rosetta(DE3) with the plasmid of N-terminal his-tagged *cyp125* gene and Rosetta2(DE3) with the plasmid of N and C- terminal his-tagged *cyp125* gene, were obtained by streaking the colonies and those were grown again in culture condition 5. This time, the soluble proteins attached to the resin were eluted by buffer D (Figure 2-6).

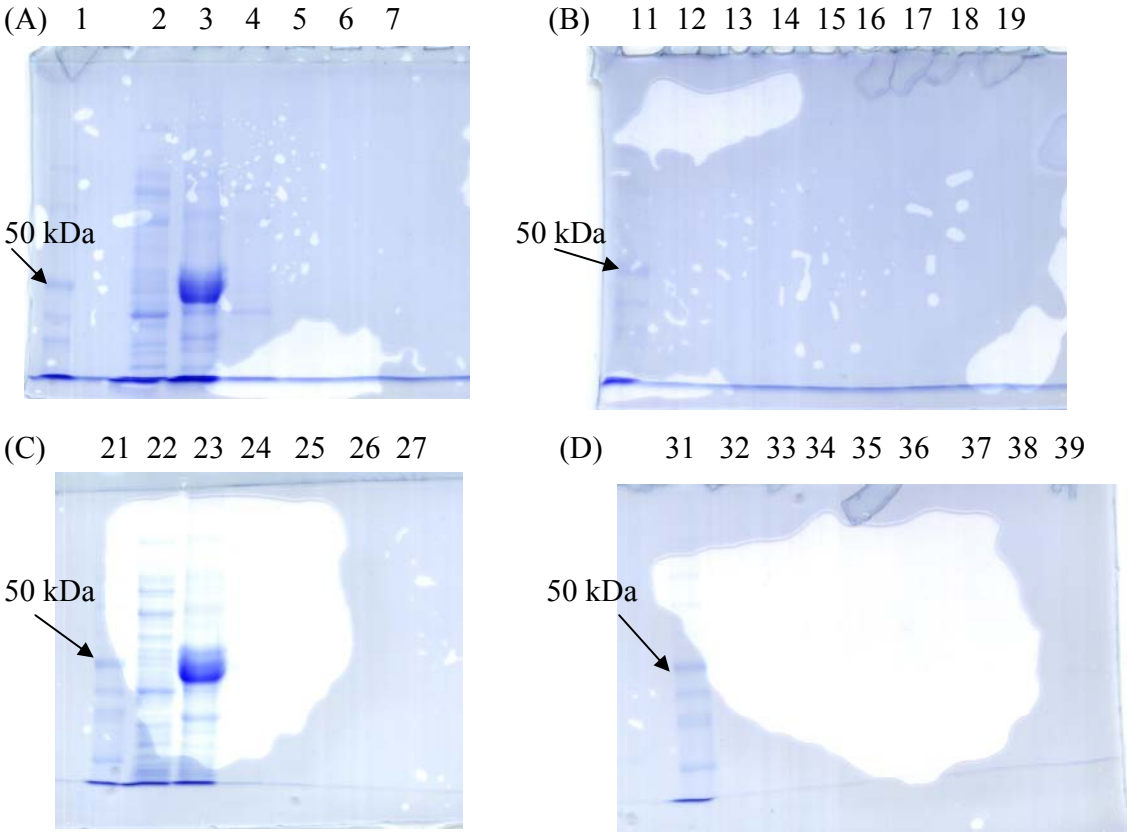

Figure 2-6 SDS-PAGE of N-terminal and N and C-terminal his-tagged CYP125s expressed in Rosetta(DE3) and Rosetta2(DE3)

(A) (B) **N-terminal his-tagged CYP125 in Rosetta(DE3)** Lane 1&11: Protein Marker, Lane 2: supernatant before TALON Metal Affinity experiment (TALON), Lane 3: pellet before TALON, Lane 4-7: wash 1-4 Lane 12-18:eluent 1-7, Lane 19: TALON resin after elution

(C) (D) **N and C-terminal his-tagged CYP125 in Rosetta2(DE3)** Lane 21&31: Protein Marker, Lane 22: supernatant before TALON, Lane 23: pellet before TALON, Lane 24-27: wash 1-4 Lane 32-38:eluent 1-7, Lane 39: TALON resin after elution

A lot of insoluble proteins were expressed again. However, there was no band of the same MW of soluble protein bands in both conditions. The red circled bands are of concern from Figure 2-5 because they are located lower than expected. Those were not the bands for CYP125. As a result, nothing was attached to and eluted from the resin.

Until now, three different plasmids (N-terminal, C-terminal, and N and C-terminal his-tagged CYP125) were transformed into three different *E. coli* competent

cells and no soluble CYP125 was expressed. So we concluded that CYP125 may not be able to be expressed in *E. coli*.

As a control, CYP121 (from Astra Zeneca) was tested. Before starting, the DNA sequence of the CYP121 plasmid was identified. The gene of CYP121 was inserted in pET15a vector but the codon frame was incorrect. This plasmid would not express the protein with the sequence of CYP121. The gene encoding CYP121 was constructed again with C-terminal his-tag in pET29a vector using *Nde* I and *Hind* III restriction sites. This newly designed plasmid was transformed into BL21(DE3)pLysS competent cells. The cells were inoculated in LB medium and grown as McLean and co-works described (*18*). After TALON metal affinity experiment, SDS-PAGE was done (Figure 2-7). The MW of CYP121 is 43 kDa and no proteins were expressed in soluble or insoluble forms.

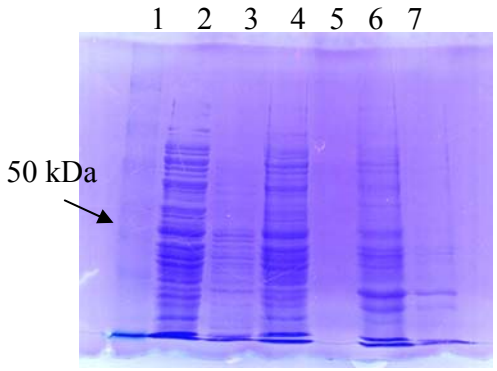

Figure 2-7 SDS-PAGE of C-terminal his-tagged CYP121 expressed in BL21(DE3)
Lane 1: protein marker, Lane 2: supernatant before TALON Metal Affinity experiment (TALON), Lane 3: supernatant after TALON, Lane 4: denatured supernatant before TALON, Lane 5: denatured supernatant after TALON, Lane 6: pellet before TALON, Lane 7: pellet after TALON

Due to the failure of CYP121 expression with the newly constructed plasmid, the original plasmid was transformed into BL21(DE3)pLysS competent cells and the cells were grown in LB medium. After induction and lysis, TALON metal affinity experiment

was carried out (Figure 2-8). No proteins were expressed at all, even in the inclusion bodies. There are two possible answers for this failure of CYP121 expression. The construct of the plasmid and the used competent cell were not same as the paper from McLean and co-works, so N-terminal his-tag and BL21(DE3) may be not suitable for expression of CYP121. Or, as DNA sequencing result shows, the original plasmid was designed incorrectly.

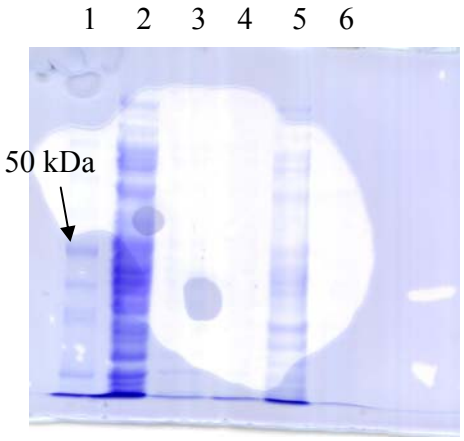

Figure 2-8 SDS-PAGE of CYP121 expressed by the original plasmid in BL21(DE3)

Lane 1: protein marker, Lane 2: supernatant before TALON Metal Affinity experiment (TALON), Lane 3: supernatant after TALON, Lane 4: denatured supernatant after TALON, Lane 5: pellet before TALON, Lane 6: pellet after TALON

We concluded that CYP125 may not be expressed in *E. coli* and therefore decided to express the protein in *M. smeg*. First, the DNA sequence of the operon, *Rv3540c-Rv3545c* in *M. tb*, was compared with *M. smeg mc*^{2}*155* using BLAST. *Rv3540c* which encodes probable lipid transfer protein or keto acyl-CoA thiolase ltp2 has 78% with MSMEG_5990 that also encodes lipid transfer protein. *Rv3541c* has 83% with MSMEG_5991 that is putative MaoC like domain. In addition, *Rv3545c* has 82% identity

with MSMEG_5995 encoding P450 thiolate protein. The genes of *Rv3542c-Rv3544c* were not found from *M. smeg* mc^2155 genome, but *M. smeg* has the genes encoding proteins functioning similarly with *M. tb* genes. *Rv3543c* and *Rv3544c* encode probable acyl-CoA dehydrogenases fadE29 and fadE28, and MSMEG_5993 and MSMEG_5994 also encodes putative acyl-CoA dehydrogenase. Moreover, as *M. tb* does, these genes are located in same operon in *M. smeg*, but the function of this operon is not identified yet.

To transform the plasmid containing *cyp125* into *M. smeg*, the gene of interest was inserted in pVV16 vector, a shuttle vector of *E. coli* and *M. smeg*. The *cyp125* gene was inserted between *Nde* I and *Hind* III restriction sites of the vector and the mutation of stop codon TAA at the end of the gene allows for expression with C-terminal his-tag. This shuttle vector carries two resistances: kanamycin and hygromycin-B. For *M. smeg*, only hygromycin-B was used as a resistance. Because the cell division time of *M. smeg* is much slower than *E. coli* (a division time of *M. smeg* is 3 h while *E. coli*'s is 20 min), it took much longer time to grow the cells. In addition, acetamide was used as an inducer of protein expression for *M. smeg*. A longer time of burst was required for *M. smeg* during sonication due to its thicker wall compared to *E. coli*. After TALON metal affinity experiment, SDS-PAGE was carried out (Figure 2-9). In lane 2 from Figure 2-9, the supernatant contains soluble protein with a MW lower than 50 kDa (red circled band). However, it was not attached to TALON resin even though the supernatant was shaken with the resin for 24 h at 4 °C. Other purification methods, but not TALON metal affinity, should be tried to purify the protein.

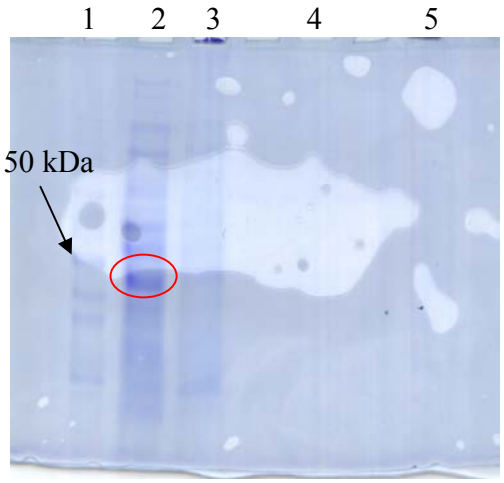

Figure 2-9 SDS-PAGE of CYP125 expressed in *M. smeg*

Lane 1: protein marker, Lane 2: supernatant before TALON Metal Affinity experiment (TALON), Lane 3: pellet before TALON, Lane 4: supernatant after TALON, Lane 5: pellet after TALON

Many different conditions were tried to express *cyp125* in *E. coli*. Three plasmids containing N-terminal, C-terminal, and N/C-terminal his-tagged *cyp125* genes were constructed in pET vectors and those plasmids were transformed into three *E. coli* competent cell strains, BL21(DE3), Rosetta(DE3), and Rosetta2(DE3). No soluble protein was expressed; however, a large amount of insoluble protein resulted. Expression of CYP121 was tried in BL21(DE3) as a control, but no expression was observed. *cyp125* was inserted in a shuttle vector, pVV16, and it was grown in *M. smeg*. A soluble protein whose MW is similar to CYP125 appeared to be expressed but metal affinity column is not appropriate for purification of the protein. We do not know whether this protein is CYP125 or not. Further investigation is needed to verify.

CHAPTER 3

Introduction of Cholesterol Oxidase

I. Overview of cholesterol oxidase

II. Type I and type II cholesterol oxidases

1. **Type I cholesterol oxidase**
2. **Type II cholesterol oxidase**

I. Overview of cholesterol oxidase

Cholesterol oxidase is a water soluble flavoenzyme that is able to catalyze the conversion of cholesterol to cholest-4-en-3-one (Scheme 3-1). It is an interfacial enzyme that binds to the surface of a membrane temporarily during catalysis. This catalyst carries out two different reactions in one active site. An oxidation of cholesterol to cholest-5-en-3-one is carried out first and an isomerization of cholest-5-en-3-one to cholest-4-en-3-one, a more thermodynamically stable intermediate, follows. During the oxidation reaction, an FAD cofactor is required as a substrate. The reduction of a FAD cofactor generates one hydride and the reduced FAD cofactor is re-oxidized by one molecule of oxygen. Then hydrogen peroxide is generated by the reduction of oxygen.

In the 1940's the oxidation of cholesterol and other sterols by microbes was reported and it was found that they utilize those sterols as their carbon source (*1*). The conversion of cholesterol to 17-keto steroids and coprostanol by microbes was noted later (*2, 3*). Since then many cholesterol oxidases have been identified in microorganisms.

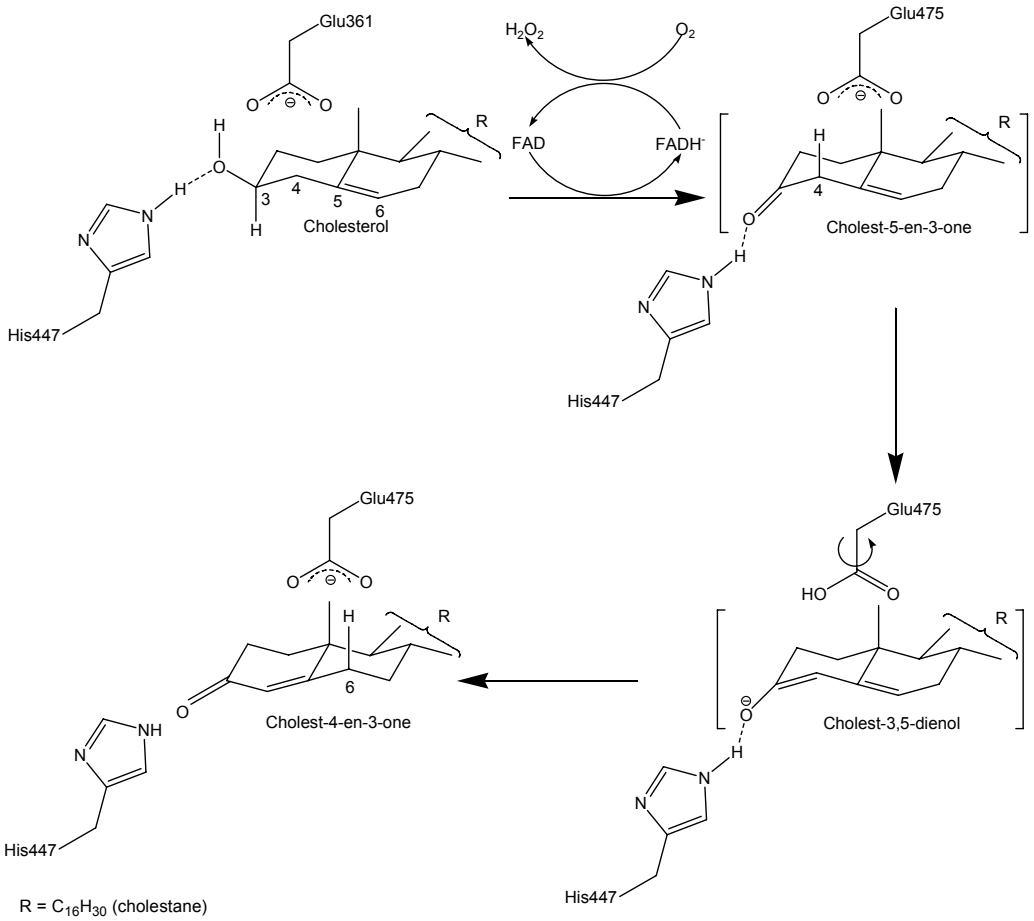

Scheme 3-1 Reaction catalyzed by cholesterol oxidases and key active site residues of type I cholesterol oxidase

The first isolation of cholesterol oxidase was from *Rhodococcus equi*, a gram-positive bacterium, in 1973 (*4*). Cholesterol oxidase was then applied in an assay for the detection of the level of serum cholesterol and utilized in clinical laboratories (*5-7*). The reaction catalyzes the conversion of cholesterol to cholest-en-3-one with the formation of biproduct hydrogen peroxide. A peroxidase, generally horseradish peroxidase, is required to reactivate the hydrogen peroxide and the reactivation of hydrogen peroxide leads to the

formation of a firmly stable colored complex detected by absorption spectrometry. This indirect detection of serum cholesterol was widely used in the diagnosis of cardiovascular diseases and arteriosclerosis that are caused by abnormal levels of serum cholesterol. Cholesterol oxidase was also used as a tool to investigate the localization of cholesterol in the plasma membrane and the heterogeneity of cell membranes in the lipid bilayer (*8-12*). Also, the presence of lipid rafts in cell membranes is somewhat proved by these research (*13*).

II. Type I and type II cholesterol oxidase

Cholesterol oxidase is a flavoenzyme that catalyzes the reactions of oxidation and isomerization in one active site. Cholesterol is oxidized to cholest-5-en-3-one and isomerized to cholest-4-en-3-one by cholesterol oxidase. Here, an FAD cofactor is required for the oxidation of cholesterol to occur.

There are two types of cholesterol oxidases, type I and type II, which are categorized by their structure homologies. Even though there are two types of cholesterol oxidases, that perform the same catalytic reaction as Scheme 3-1, these different types carry out distinct catalytic mechanism based on different kinetic properties and redox potentials (*14*).

1. Type I cholesterol oxidase

The three-dimensional structures of two type I cholesterol oxidases has been solved. These cholesterol oxidases are from *Streptomyces sp.* SA-COO and *R. equi* (*15-17*). The amino acid sequences of these two oxidases are almost identical and the structures are nearly same. An FAD cofactor is required for the oxidation reaction which binds noncovalently to type I cholesterol oxidase. The conserved active sites of the cholesterol oxidases were revealed by their crystallographic structures. The oxidases are classified as the members of the GMC (glucose-methanol-choline) oxidoreductase family of flavoenzymes due to the noncovalently bound FAD to the enzyme. The enzymes of the GMC oxidoreductase family need the FAD cofactor and oxidize a hydroxyl group to a ketone. His447 and Asn485 are semiconserved in the enzymes that seem to be important in substrate oxidation (*18*).

Conservation of His447 in the GMC oxidoreductase family has been proven by sequence and structure alignments of the active site (*16*). Also, the importance of this residue is revealed by the mutagenesis and kinetic studies (*17, 19*). In cholesterol oxidase, His447 is a hydrogen bond donor to the hydroxyl oxygen atom of the substrate. It helps the substrate position with respect to the flavin, too. The side chain of Glu361 is exposed to the hydrogen atom of the steroid hydroxyl group in this arrangement. Then the protonated NE2 of His447 faces the lone pair of electrons.

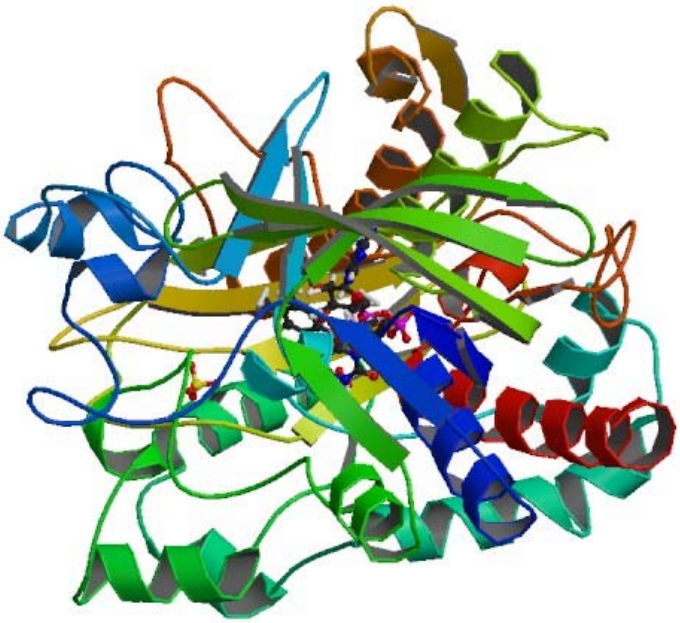

Figure 3-1 Atomic resolution structure of cholesterol oxidase from *Streptomyces sp.* SA-COO (Type I cholesterol oxidase). The FAD cofactor is showed as a ball-and-stick model (*20*).

A bound steroid to the enzyme was observed from a complex of the reduced enzyme and dehydroepiandosterone in a buried active site with a bound water molecule (Wat541) close to the hydroxyl group (*16*). The X-ray structure of the *Streptomyces* cholesterol oxidase to sub-Ångstrom resolution (0.95 Å) suggests a new model for the Michaelis complex that the Wat541 mimics the substrate hydroxyl group (*20*).

The isomerization of cholest-5-en-3-one to cholest-4-en-3-one by cholesterol oxidase, a second nonredox reaction that takes place in the active site, is unique from other GMC family members. Deuterium transfer and mutagenesis studies found out that

this reaction is a base-catalyzed process (*21-23*). The 4*β* hydrogen is moved to the 6*β* position on the steroid (*21, 22*) and this isomerization is catalyzed by Glu361 positioned over the *β*-face (*16, 17*).

Another semiconserved residue in the active site, Asn485, is deeply involved in the oxidation of cholesterol oxidase. An electron potential is created around the FAD cofactor by the amide-*π* interaction between the asparagines side chain and the *π*-system of the pyrimidine of the FAD cofactor and it has stabilization energy (*24*). This stabilization enhances the oxidation reaction.

2. Type II cholesterol oxidase

Type II cholesterol oxidase is from *Brevibacterium Sterolicum* and it is structurally distinct from Type I cholesterol oxidase. Even though it carries out the identical catalytic reaction as Type I cholesterol oxidase, the way of binding FAD cofactor is different: Type II cholesterol oxidase has a covalently bound FAD cofactor via a histidine residue while Type I enzyme has a noncovalently bound FAD cofactor (*25, 26*). These two types of cholesterol oxidases have different redox potential and kinetic properties and this makes the enzymes have different mechanisms of oxidation. The midpoint reduction potential of type II cholesterol oxidase is -101 mV (*27*) while type I enzyme's is -278 mV (*24*). By comparing the values of type I and type II enzymes, type II cholesterol oxidase is able to perform the thermodynamic reduction of the FAD cofactor more favorably than type I cholesterol oxidase which means that type II enzyme is a better oxidizing agent.

Type II cholesterol oxidase has a much more hydrophilic active site compared to type I enzyme. There are four glutamate residues (Glu475, Glu551, Glu432, and Glu311), an arginine (Arg477), a lysine (Lys554), and an asparagine (Asn516) in the pyrimidine region of the active site cavity of the type II enzyme. For type I cholesterol oxidase, there are only three polar residues in the active site: Glu361, His447, and Asn485.

Figure 3-2 Crystal structure of cholesterol oxidase from *Brevibacterium* (Type II cholesterol oxidase). The FAD cofactor is showed as a ball-and-stick model (*16*).

CHAPTER 4

Labeling Wild-Type Cholesterol Oxidase with ^{2}H, ^{13}C, and ^{15}N for Structural Characterization

I. Introduction

II. Materials and methods

III. Results and discussion

I. Introduction

ChoA is classified as the GMC oxidoreductase family of enzymes. These enzymes utilize the FAD cofactor and catalyze oxidation of a hydroxyl group to a ketone. Glucose oxidase has a homologus structure with cholesterol oxidase and it catalyzes the oxidation reaction. Residues 441-491 of ChoA are categorized as the GMC oxidoreduxtase domain (CDD # 45101) and are involved in the formation of its catalytic center. The substrate-binding domain of the enzyme is mostly composed of α helixes and β sheets and the substrate binding loops are on a single face. There are two substrate binding loops: residues 78-87 form loop 1 and residues 433-436 are loop 2. These loops are flexible due to the poor electron density in the region and ChoA is able to make opened and closed conformational changes during its catalytic cycle. These loops cap the active site of the protein and we postulate that a hydrophobic pathway is formed between the active site and the membrane by opening the loops.

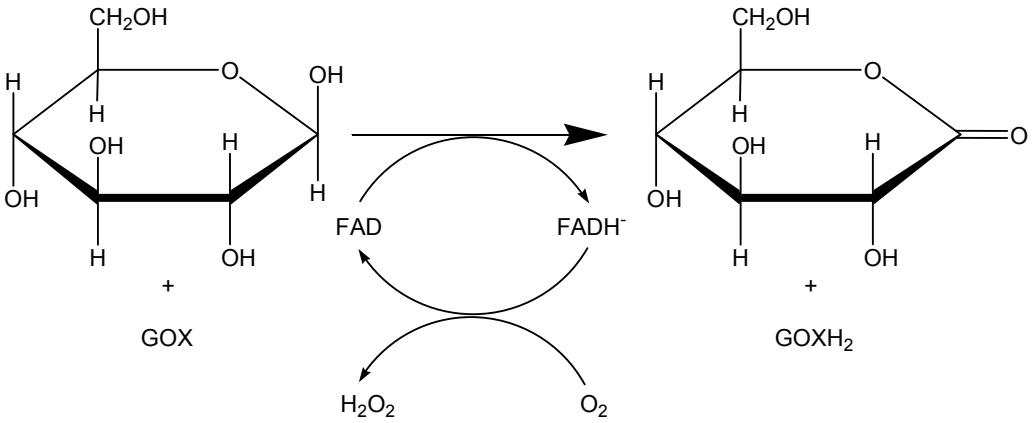

Scheme 4-1 The enzyme reaction catalyzed by glucose oxidase

In general, the mobility of a loop is revealed by X-ray structural analysis. When an enzyme is crystallized in different loop conformations, with and without its substrate, this can be the important evidence that the loop is involved in the catalytic reaction of the enzyme. Nuclear magnetic resonance (NMR) spectroscopy is also able to support the importance of dynamics of proteins. NMR is generally used to explain macromolecular dynamics (*1*). However, it is hard to get high-quality spectra as the size of molecules gets larger, and sensing the motion of molecules is limited in NMR experiment by the narrow time scale. NMR spin-relaxation experiments somewhat solved these problems in small proteins (*2, 3*). The problem is that natural proteins are usually large and its conformational exchange rate might be broad (molecular weight of ChoA is ~57 kDa). The utilization of ^{15}N relaxation with an off-resonance spin-lock field made quantification of fast conformational exchange processes in large protein possible (*4*).

The aim of this research is to label WT ChoA with ^{2}H, ^{13}C, and ^{15}N to determine whether the spectrum of WT ChoA is sufficiently resolved for residue assignment and protein dynamic measurements by NMR.

II. Materials and Methods

Materials

$^{15}NH_4Cl$ and D_2O were purchased from Cambridge Isotope Laboratories, Inc. (Andover, MA). D-glucose-$^{13}C_6$ and MEM Vitamin solution (100X) were from ISOTEC (Milwaukee, WI) and Thermo Scientific HyClone (Logan, Utah), respectively. Albumin bovine serum (BSA), min 99% and Triton X-100 were purchased from Sigma-Aldrich (St. Louis, MO). Cholesterol (5-cholesten-3β-ol), +99% was from Sigma Chemical Co. (St. Louis, MO). IPTG was from Anatrace (Maumee, Ohio). All other chemical reagents were purchased from Fisher Scientific (Pittsburgh, PA). Water used for assays and chromatography was distilled by Barnstead NANOpure ultrafilter system.

Buffers and media

500 mM sodium phosphate buffer (pH 7.0): 24.81 g $NaH_2PO_4 \cdot H_20$, 45.55 g Na_2HPO_4 in 1 L DDI H_2O; Buffer E: 50 mM sodium phosphate buffer; Buffer F: 2 M $(NH_4)_2SO_4$; Luria broth (LB) medium: 20 g LB in 1 L DDI H_2O; M9 minimal medium for labeling ^{15}N: 6.8 g Na_2HPO_4, 3.0 g KH_2PO_4, 0.5 g NaCl, 1.0 g $^{15}NH_4Cl$, 4.0 g D-glucose, 100 μL 1.0 M $CaCl_2$, 1.0 mL 2 M $MgSO_4$ in 1L DDI H_2O; M9 minimal medium for labeling ^{2}H, ^{13}C, and ^{15}N: 6.8 g Na_2HPO_4, 3.0 g KH_2PO_4, 0.5 g NaCl, 1.0 g $^{15}NH_4Cl$, 4.0 g ^{13}C-labeled glucose, 100 μL 1.0 M $CaCl_2$, 1.0 mL 2 M $MgSO_4$, 10 mL MEM vitamin solution (100X) in 1L 100% D_2O; 2XYT medium: 16 g tryptone, 10 g yeast extract, 5 g NaCl in 1 L DDI H_2O

Methods

Expression of ^{15}N labeled WT ChoA

The gene encodes for WT ChoA in the pCO117 (*5*) vector was transformed into *E. coli* strain BL21(DE3)pLysS competent cells. A LB-agar plate containing 200 μg/mL ampicillin was used to grow colonies of transformed cells. The plate was placed at 37 °C overnight. A single colony was inoculated in 10 mL of LB medium, containing 200 μg/mL ampicillin, in a sterilized transformation tube at 37 °C and 250 RPM overnight. 1 ml of the inoculated culture was taken to inoculate a 25 mL M9 minimal medium with and it was grown until an $O.D._{600} = 0.6$ at 37 °C and 250 RPM (standard condition). The inoculated M9 culture was centrifuged at 4,000 X *g* for 20 min (4 °C) and the pellet was resuspended and inoculated in a 1 L M9 minimal medium containing 200 μg/mL ampicillin. This culture was grown under standard conditions. The temperature was decreased to 28 °C and the culture was allowed to equilibrate. The inoculated culture was then induced by addition of 0.4 mM IPTG and incubated for 16 h. The cells were pelleted by centrifugation at 4,000 X *g* for 20 min (4 °C).

Expression of ^{2}H, ^{13}C, ^{15}N labeled WT ChoA

The gene encodes for WT ChoA in the pCO117 (*5*) vector was transformed into *E. coli* strain BL21(DE3)pLysS competent cells. A LB-agar plate containing 200 μg/mL ampicillin was used to grow colonies of transformed cells. The plate was placed at 37 °C overnight. A single colony was inoculated in 10 mL of LB medium, containing 200 μg/mL ampicillin, in a sterilized transformation tube at 37 °C and 250 RPM overnight. 1 ml of the inoculated culture was taken to inoculate a 25 mL M9 minimal medium with 50% D_2O, and it was grown until an $O.D._{600} = 0.6$ at 37 °C and 250 RPM (standard

condition). The inoculated M9 culture was centrifuged at 4,000 X *g* for 20 min (4 °C) and the pellet was resuspended and inoculated in a 250 mL M9 minimal medium with 70% D_2O containing 200 μg/mL ampicillin. This culture was grown under standard conditions until an $O.D._{600}$ = 0.6. The inoculated M9 culture was centrifuged at 4,000 X *g* for 20 min (4 °C) and the pellet was resuspended and inoculated in 1 L M9 minimal medium with 100% D_2O containing 200 μg/mL ampicillin. This culture was grown under standard conditions. The temperature was decreased to 28 °C and the culture was allowed to equilibrate. The inoculated culture was then induced by addition of 0.4 mM IPTG and incubated for 16 h. The cells were pelleted by centrifugation at 4,000 X *g* for 20 min (4 °C).

Purification of WT ChoA

Cell paste from M9 minimal culture was resuspended in small volume of buffer E. Cells were broken by a French press (~18,000 psi., three times) and the lysate was ultracentrifuged at 135,000 X *g* for 1 h (4 °C). The pellet was discarded and the supernatant was precipitated by 1.0 M ammonium sulfate. After the centrifugation at 4,000 X *g* for 20 min (4 °C), the pellet was discarded. The final ammonium sulfate concentration of the supernatant was 2.0 M and it was centrifuged at 4,000 X *g* for 20 min (4 °C). The pellet was resuspended in small volume of buffer E and dialyzed (MWCO 6,000-8,000) against 2 L buffer E three times. The dialyzed pellet was loaded onto a DEAE-cellulose (30 mm X 25 cm, DE-52, Whatman) column, pre-equilibrated in buffer E. The WT ChoA-containing fractions (determined by UV assay) were eluted with buffer E and combined together. The combined fractions were precipitated by 2.5 M ammonium sulfate and centrifuged at 4,000 X *g* for 20 min (4 °C). The supernatant was

discarded and the pellet was resuspended in a minimal volume of buffer E. The protein was loaded onto a butyl Sepharose column (30 ml butyl-Sepharose-4 Fast Flow, XK 16/40, Pharmacia Biotech, Upsala, Sweden), pre-equilibrated with buffer F. The column was developed by a linear gradient of 75% buffer F to 100% buffer E (200 ml). The elution profile was monitored by UV absorbance at 280 nm and the presence of ChoA was configured by UV assay. The fractions containing WT ChoA were combined together and adjusted the volume to 50 mL with buffer E. Amicon ultra-centrifugal filter (YM30 membrane) was carried out for three times to exchange the buffer to buffer A and concentrate the protein.

Preparation of vesicles

POPC (1-palmitoyl-2-oleoyl-sn-glycero-3-phosphochlorine) and cholesterol were prepared in chloroform in 7:3 ratios, respectively, and the final concentration of the lipid was 18 μM. The mixture was transferred into a round-bottom flask and dried as a thin film under reduced pressure in a rotary evaporator. It was evacuated under high vacuum overnight. The lipids were resuspended in 6 mL buffer E with vortexing. After five freeze thaw cycles, at -80 °C and 37 °C, 10 extrusion cycles were followed through two stacked 100 nm filters using a nitrogen gas pressure of 350-400 psi.

Assessment of WT ChoA

Protein-containing fractions were determined by 12% SDS-PAGE at different steps of the purification procedure. The presence of WT ChoA was determined by UV assay, when the formation of cholest-4-en-3-one was monitored at 240 nm (ε_{240} = 12,100 $M^{-1} \cdot cm^{-1}$ for cholesterol). 0.025 % (w/v) Triton X-100 and 0.02 % (w/v) BSA were added to buffer E, and cholesterol was added as a propan-2-ol solution. The amount of WT

ChoA that finally obtained was determined by the UV absorbance at 280 nm (ε_{280} = 81,924 $M^{-1} \cdot cm^{-1}$ for WT ChoA). For the UV assays, a Shimadzu UV2101 PC Spectrophotometer was used. The sizes of WT ChoA and POPC/cholesterol vesicles were assessed by 90 Plus Particle Size Analyzer (Brookhaven Instruments Corporation). The conformational change of WT ChoA was determined by HSQC (700 MHz) at 25 °C.

Recycling D_2O (*6*)

Visible debris from the used M9 minimal medium with 100 % D_2O was removed by centrifuge at 4,000 X *g* for 20 min (at 4 °C) and filtering. Using rotary evaporator, D_2O was rotary evaporated three times. The distilled D_2O was mixed with activated charcoal and stirred for 20 min. the charcoal was removed by filtration from D_2O.

III. Results and discussion

To practice the expression and purification of WT ChoA, construct pCO202 (*7*) in which the gene encoding for WT ChoA was subcloned into, was transformed into *E. coli* strain BL21(DE3)pLysS competent cells and it was grown in 2XYT medium at 37 °C. When the $O.D._{600}$ = 0.6, the temperature was decreased to 28 °C and 0.4 mM IPTG was added to the culture. It was induced for 8 h. WT ChoA was purified using the same procedure described in methods. Finally, approximately 12 mg of WT ChoA was obtained from 5 L 2XYT medium while our former group members had obtained ~50 mg of the protein from 1 L 2XYT medium. The low yield of WT ChoA was due to the plasmid. pCO202 plasmid was constructed to increase the yield of plasmid when the protein was mutated (*7*). The mutation was carried out by cassette mutagenesis using pCO202 and the lower level of mutant cholesterol oxidase was expressed heterologously in *E. coli* than wild-type cholesterol oxidase. For that reason, the yield of purified WT ChoA from pCO202 was low.

M9 minimal medium is used for growing bacteria to get suitable proteins with isotope labeled for NMR analysis. The medium contains a minimum amount of nutrients so that bacteria can grow. This however decreases the amount of protein that can be obtained from M9 minimal medium compared to 2XYT medium. For that reason, pCO117 into which the WT ChoA was subcloned was used to get the maximum amount of WT ChoA.

To determine the appropriate induction temperature and time for expressing WT ChoA in M9 minimal medium, two cultures were induced at different temperatures (28 °C and 37 °C). 2 mL samples were collected every 4 h from 16 h post induction. The

samples were sonicated and centrifuged. The supernatants were assayed using cholesterol as a substrate (Figure 4-1).

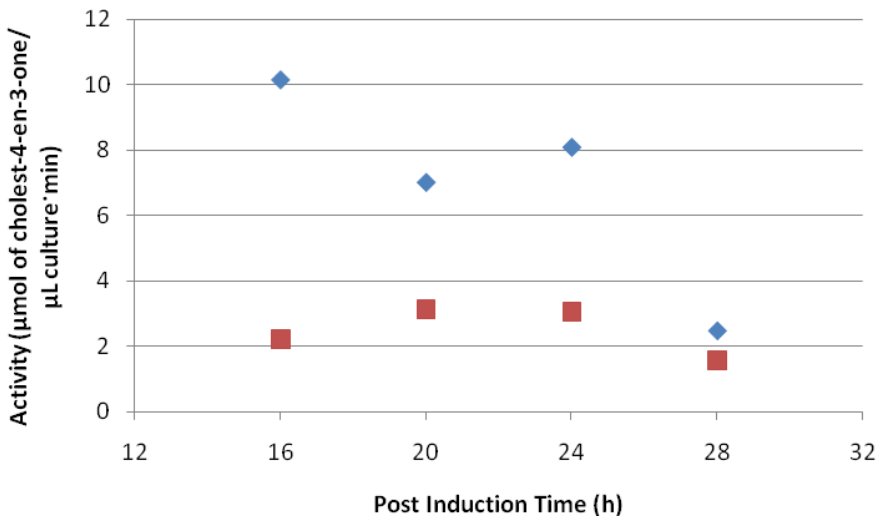

Figure 4-1 Activity of WT ChoA depending on post induction time and temperature. ♦ indicates the activity of WT ChoA induced at 28 °C when the protein was UV assayed with cholesterol; ■ indicates the activity of WT ChoA induced at 37 °C

The proteins induced at 28 °C showed higher activity than those induced at 37 °C. This means that the overexpression level of *choA* is better at 28 °C in the same amount of culture. According to the result, the suitable temperature for the induction of WT ChoA in M9 minimal medium is 28 ºC. However, the activity kept decreasing from 16 h post induction at 28 °C. So, M9 minimal culture containing cells were grown again in 28 ºC and 2 ml samples were collected every 4 h from 8 h post induction (Figure 4-2).

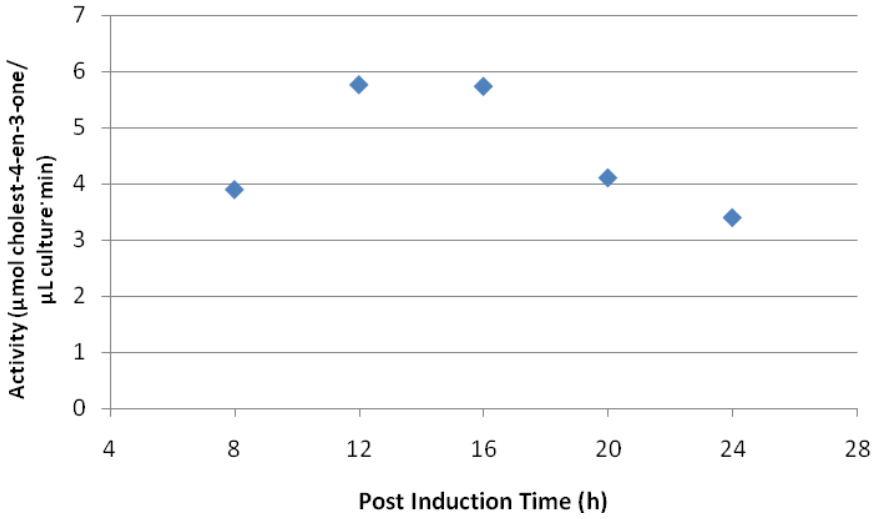

Figure 4-2 Activity of WT ChoA depending on post induction time

The activity increases from 8 h post induction and becomes stable at 12-16 h post induction. The decrease in the initial velocity occurs from 20 h post induction. This result indicates that the proper induction time for WT ChoA in M9 minimal medium is 12-16 h.

Once optimum conditions for expression in M9 minimal medium were obtained, ^{15}N labeled ammonium chloride was used; which allows for isotope labeling of ChoA. 4.61 mg of purified ^{15}N labeled ChoA was obtained from 1 L of culture. The size of the ChoA was assassed by Light Scattering and it was approximately 6 nm which means that it was not aggregated. The 2D ^{1}H-^{15}N HSQC was obtained for ^{15}N labeled ChoA (160 µM) at 25 °C (Figure 4-3). After the preparation of 6 mM POPC/cholesterol vesicles, the size of the vesicles was measured by Light Scattering and it was approximately 100 nm. The 2D ^{1}H-^{15}N HSQC was obtained for ^{15}N labeled ChoA (120 µM) with POPC/cholesterol vesicles (500 µM) (Figure 4-4). Changes observed in the HSQC

spectra could be utilized to identify conformational changes of the protein upon binding to cholesterol liposomes.

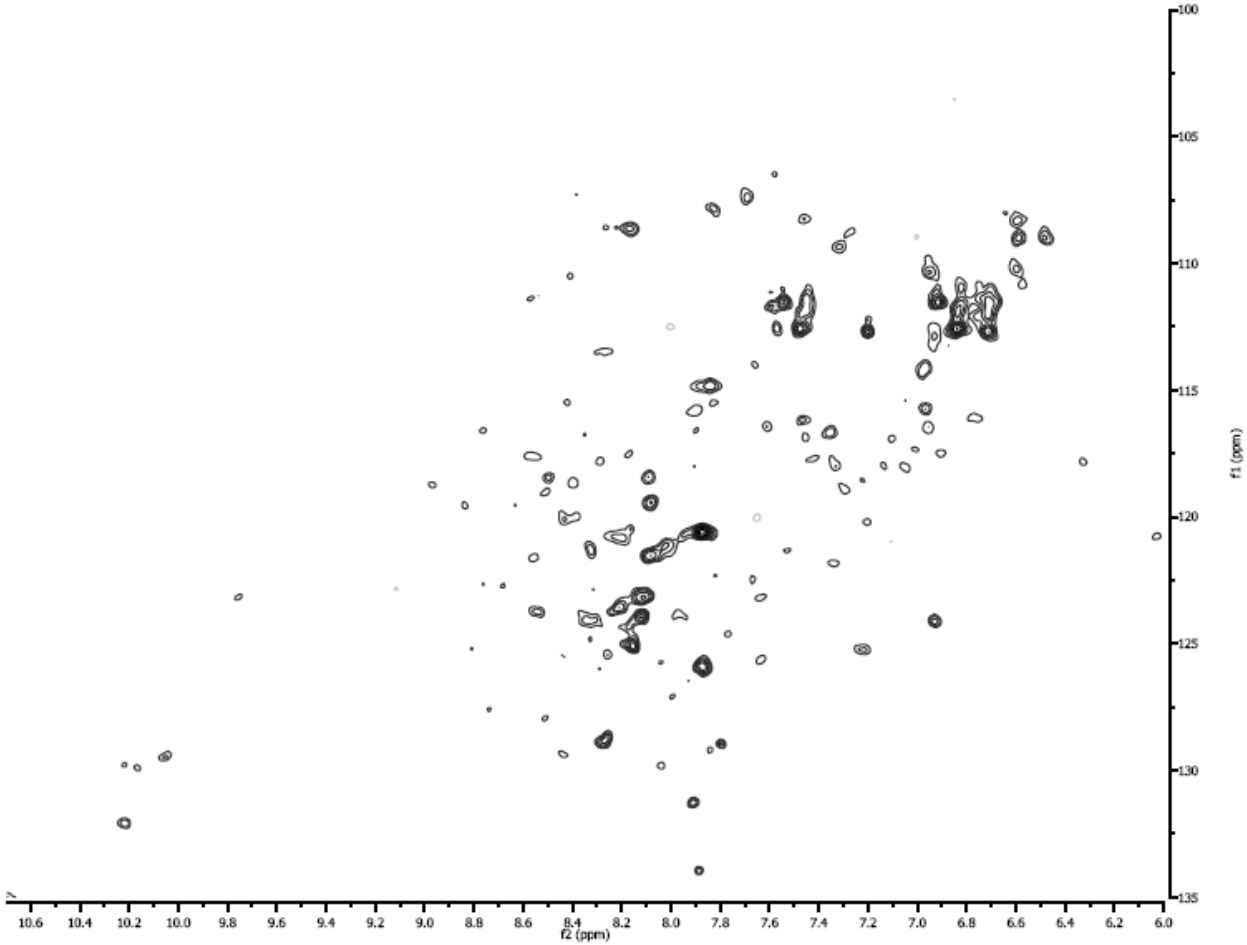

Figure 4-3 Superimposed 2D (^{1}H-^{15}N) HSQC (700 MHz) spectra of uniformly ^{15}N labeled WT ChoA recorded in a mixed solvent of 90% H_2O and 10% D_2O at 25 °C and pH 7.0.

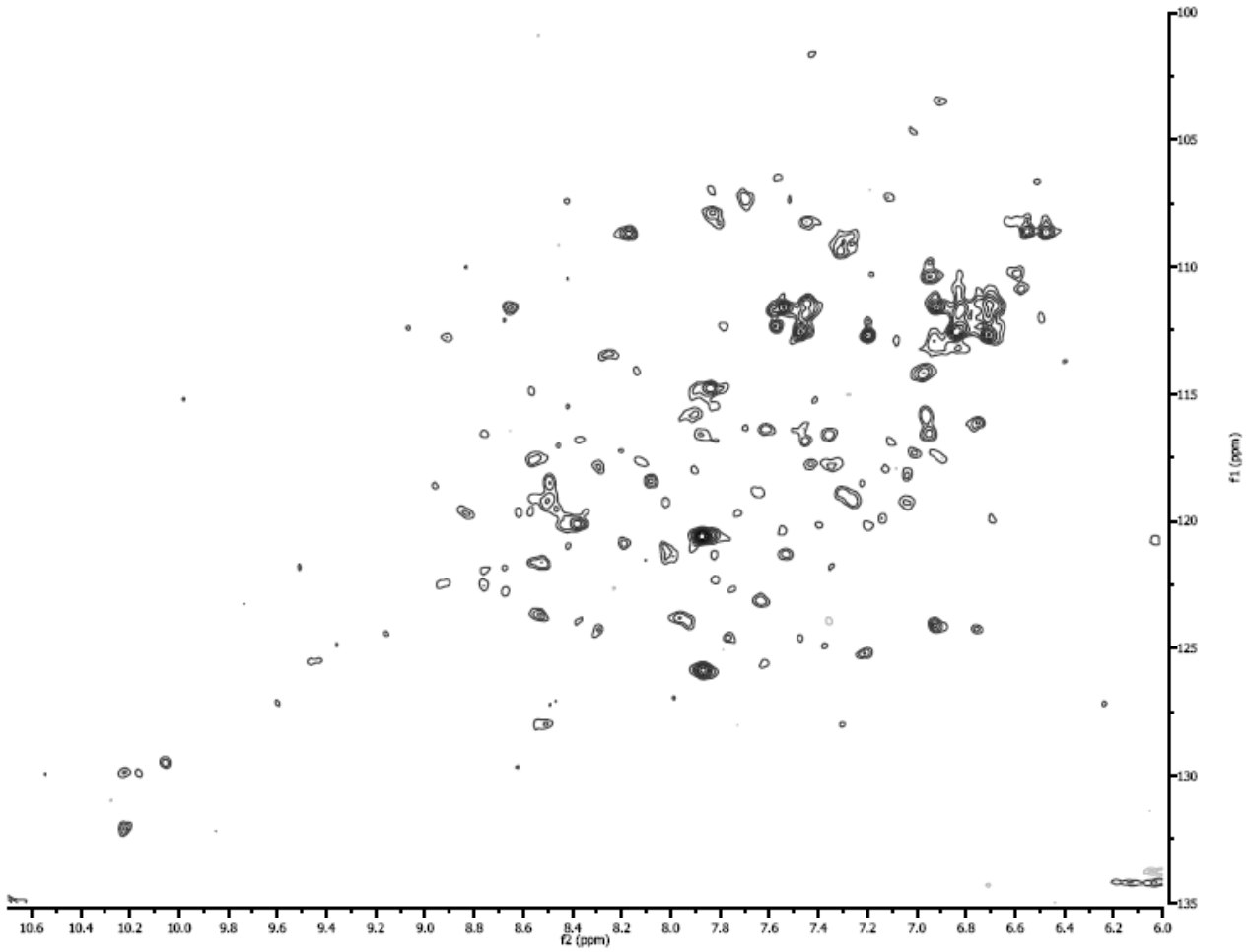

Figure 4-4 Superimposed 2D (^{1}H-^{15}N) HSQC (700 MHz) spectra of uniformly ^{15}N labeled WT ChoA with vesicles recorded in a mixed solvent of 90% H_2O and 10% D_2O at 25 °C and pH 7.0.

Those two spectra were stacked together in Figure 4-5. Green and red peaks represent WT ChoA and the protein with vesicles, respectively. Generally, some peaks overlap each other; however, some other peaks disappeared or shifted after the addition of vesicles to the protein. These shifts revealed that the residues in the active site of WT ChoA made conformational changes when the vesicles bound to the protein. Further analysis is needed to assign the peaks and characterize the three-dimensional structure and dynamics of WT ChoA accurately.

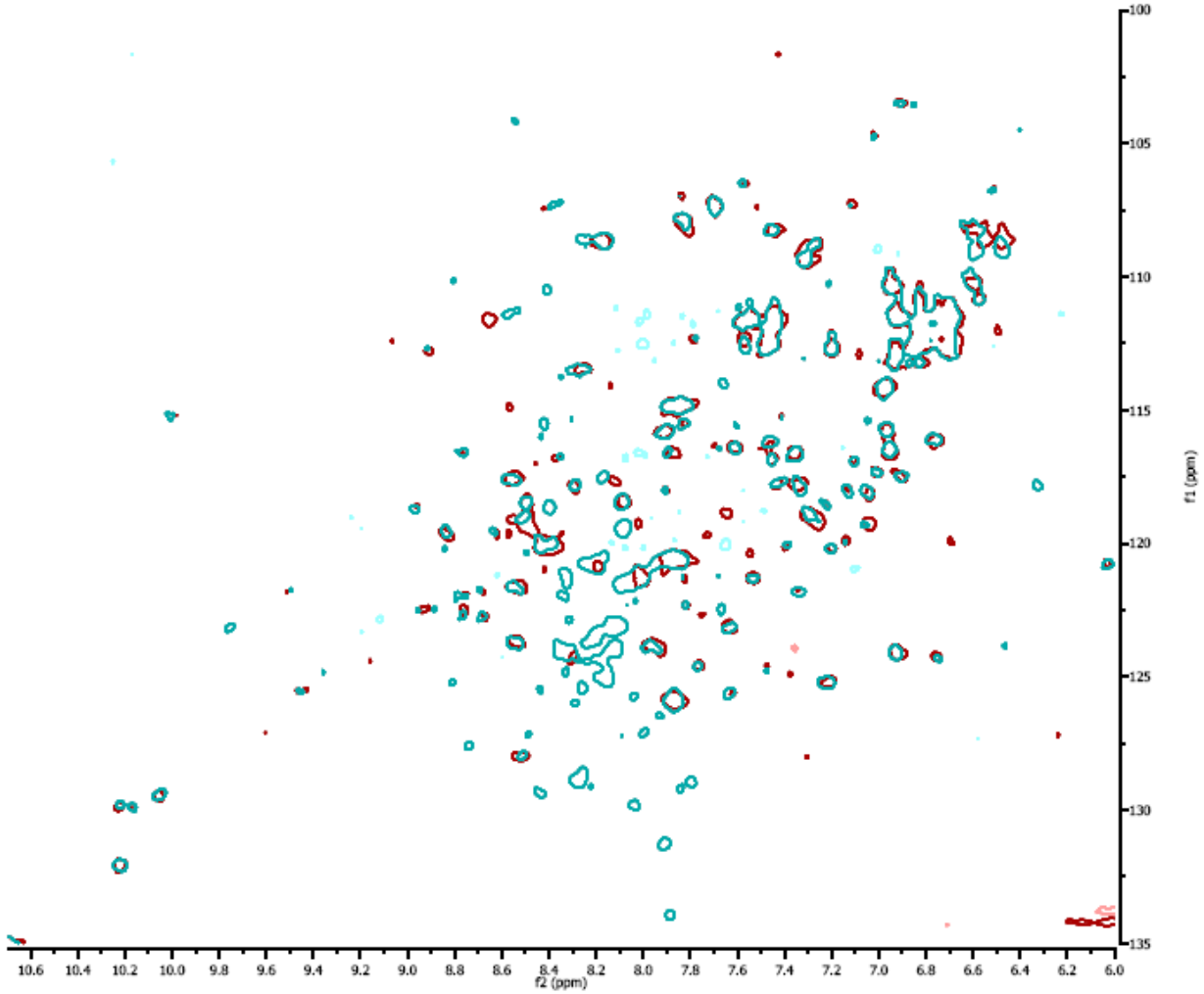

Figure 4-5 Stacked ^{1}H-^{15}N HSQC (700 MHz) data of WT ChoA and WT ChoA with vesicles. Green line represents the data of WT ChoA only and red line represents the data of WT ChoA with vesicles.

It is necessary to label ^{2}H, ^{13}C, and ^{15}N proteins in order to utilize NMR techniques for conformational analysis. Therefore, ^{15}N labeled ammonium chloride, $^{13}C_6$ D-glucose, and D_2O were used in M9 minimal medium in this experiment. In addition, MEM vitamin was added to the medium. Expression and purification were done as described in methods. However, there was a time difference for cell growth to mid-log phase between M9 minimal medium with 100% DDI H_2O and 100% D_2O. When WT ChoA was grown in M9 medium with 100% DDI H_2O, 1 mL inoculated LB culture was transferred to 25 mL M9 medium and it took approximately 3 h to reach the culture to the mid-log phase. The cells were harvested and grown in 1 L M9 medium for approximately 8 h to $O.D._{600}$ = 0.6. On the other hand, it took much longer time to grow the cells in M9 medium with 100% D_2O. The time necessary to reach mid-log phase in 25 mL M9 medium was similar. When the cells were harvested and transferred to 250 mL M9 medium with 70% D_2O, it took approximately 14 h to reach the culture to the mid-log phase. This huge time difference is due to ^{2}H, but was not observed for ^{13}C and ^{15}N labeling. Usually the chemical behavioral differences between isotopes are far too small or even detect, but it is not for deuterium. The rate of bond energy changes in deuterium is larger than other isotopes due to the small size of the atom. Also, the viscosity of D_2O is much larger than H_2O. The cells utilize H_2O as they metabolize, however, D_2O disrupts the normal metabolism of the cells. Consequently, the cells require more time to adapt to the environmental changes. The cells were harvested and resuspended in 1 L M9 medium with 100% D_2O. While the cells were inoculated in 1 L M9 culture with 100 % D_2O, the labeled ^{1}H in the protein was exchanged to ^{2}H. However, the value of $O.D._{600}$ was never changed from 0.350 for 3 days. The unchanged $O.D._{600}$

value indicates that the cell division is not occurring and this was continued at 37 °C for 3 days. This may cause abnormality to the cells. To grow the cells more, 50 mL DDI H_2O was added to the medium on the 3rd day but the absorbance did not change for 12 h. Then, 0.4 mM IPTG was added to the medium and it was induced for 16 h.

After lysis and ultracentrifugation, SDS-PAGE was run to determine the presence of WT ChoA during ammonium sulfate precipitation and dialysis (Figure 4-6). According to SDS-PAGE, there was the protein with a larger MW than unlabeled WT ChoA in the supernatant after ultracentrifuge. Also, after 2 M precipitation, the protein with larger MW than unlabeled protein was presented in the dialyzed pellet. Labeling ^{2}H, ^{13}C, and ^{15}N to the protein makes its MW heavier than the unlabeled protein.

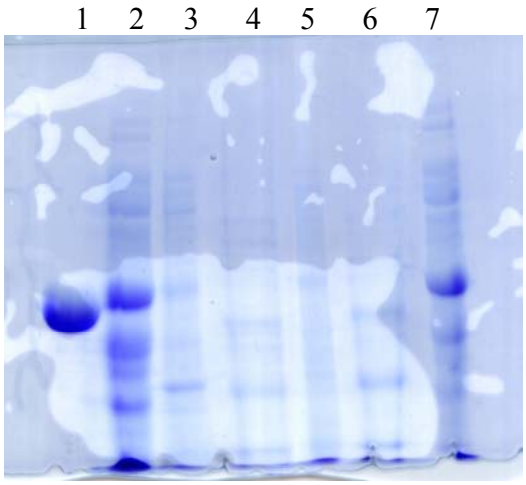

Figure 4-6 SDS-PAGE in precipitation and dialysis steps.
Lane 1: unlabeled WT ChoA; Lane 2: supernatant after lysis and ultracentrifugation; Lane 3: pellet after lysis and ultracentrifugation; Lane 4: supernatant after precipitation by 1M $(NH_4)_2SO_4$; Lane 5: pellet after precipitation by 1M $(NH_4)_2SO_4$; Lane 6: supernatant after precipitation by 2M $(NH_4)_2SO_4$; Lane 7: pellet after precipitation by 2M $(NH_4)_2SO_4$ and dialysis

WT ChoA was purified by DE-52 column and the presence of the protein was easily distinguishable by the yellow fraction color due to the presence of FAD. UV assay was carried out with 20 µL of the fractions to determine the fractions containing the protein accurately. After 2.5 M ammonium sulfate precipitation, WT ChoA was further purified by butyl-sepharose column by FPLC. The UV detector (A_{280}) in FPLC determined which fractions contained WT ChoA and the fractions were UV assayed again. The protein was concentrated by Amicon ultrafiltration to 500 µL and its final concentration was determined by UV absorbance at 280 nm (Figure 4-7).

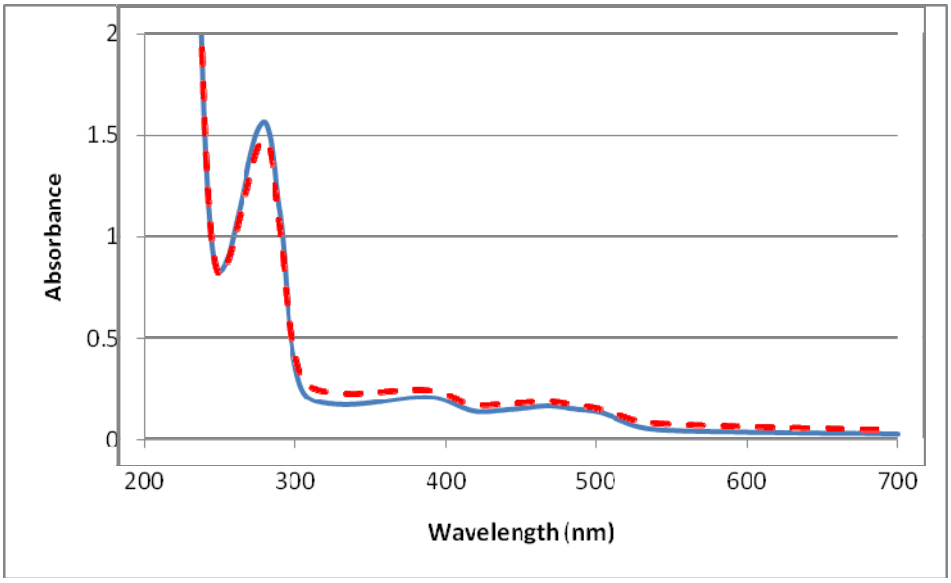

Figure 4-7 Stacked UV spectrum of purified ^{2}H, ^{13}C, ^{15}N labeled WT ChoA and unlabeled WT ChoA

- - - represents ^{2}H, ^{13}C, ^{15}N labeled WT ChoA and ——— represents unlabeled WT ChoA

The final yield of labeled WT ChoA was calculated by Beer's Law (ε_{280} = 81,924 M^{-1} cm^{-1}, MW = 57 kDa for WT ChoA). At 280 nm, the absorbance was 1.478 and 2.57 mg of ^{2}H, ^{13}C, ^{15}N labeled WT ChoA (90.2 mM) was obtained from 1 L M9 minimal culture. The UV spectrum of ^{2}H, ^{13}C, ^{15}N labeled WT ChoA is stacked with that of unlabeled WT ChoA in Figure 4-7 and the pattern of absorbance change between these two spectra is identical. The specific activity of ^{2}H, ^{13}C, ^{15}N labeled WT ChoA was 935 μmol of cholest-4-en-3-one/mg of ^{2}H, ^{13}C, ^{15}N labeled WT ChoA·min which is similar to that of unlabeled protein (992 μmol of cholest-4-en-3-one/mg of unlabeled WT ChoA·min). This protein was sent to our cooperated lab (Dr. Nicolas Doucet and Prof Patrick Loria, Yale University), and they took the ^{1}H-^{15}N 2D TROSY of ChoA. The spectrum is shown in Figure 4-8. Even though it is still good, the more concentrated protein or a higher field with a cryoprobe NMR is required to get a good enough 3D to assign the residue of the protein.

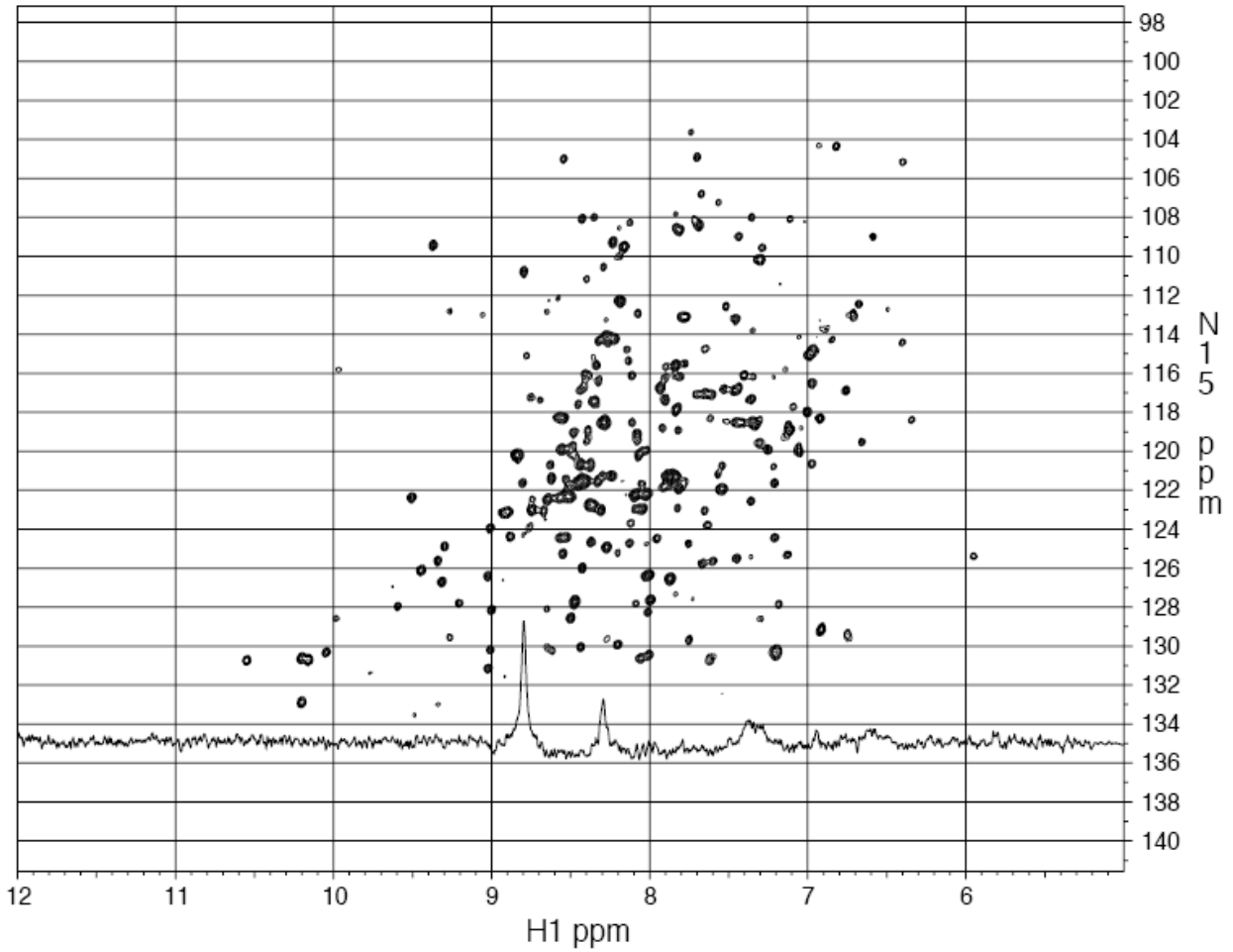

Figure 4-8 2D (^{1}H-^{15}N) TROSY (600 MHz) spectra of uniformly ^{2}H, ^{13}C, ^{15}N labeled WT ChoA (Dr. Nicolas Doucet and Prof Patrick Loria, Yale University)

References

CHAPTER 1

1. Kochi, A. (1991) The global tuberculosis situation and the new control strategy of the World Health Organization, *Tubercle 72*, 1-6.
2. WorldHealthOrganization. http://www.who.int/mediacentre/factsheets/fs104/en/index.html.
3. Byarugaba, D. K. (2004) A view on antimicrobial resistance in developing countries and responsible risk factors, *International journal of antimicrobial agents 24*, 105-110.
4. Mwinga, A., and Bernard Fourie, P. (2004) Prospects for new tuberculosis treatment in Africa, *Trop Med Int Health 9*, 827-832.
5. (2006) XDR-TB--a global threat, *Lancet 368*, 964.
6. Raviglione, M. C., and Smith, I. M. (2007) XDR tuberculosis--implications for global public health, *The New England journal of medicine 356*, 656-659.
7. Rattan, A., Kalia, A., and Ahmad, N. (1998) Multidrug-resistant Mycobacterium tuberculosis: molecular perspectives, *Emerging infectious diseases 4*, 195-209.
8. Cohen, J. (2006) Infectious disease. Extensively drug-resistant TB gets foothold in South Africa, *Science 313*, 1554.
9. Marris, E. (2006) Extreme TB strain threatens HIV victims worldwide, *Nature 443*, 131.
10. Clemens, D. L. (1996) Characterization of the Mycobacterium tuberculosis phagosome, *Trends Microbiol 4*, 113-118.
11. Barker, L. P., George, K. M., Falkow, S., and Small, P. L. (1997) Differential trafficking of live and dead Mycobacterium marinum organisms in macrophages, *Infection and immunity 65*, 1497-1504.
12. Pieters, J. (2001) Entry and survival of pathogenic mycobacteria in macrophages, *Microbes and infection / Institut Pasteur 3*, 249-255.
13. Cole, S. T., Brosch, R., Parkhill, J., Garnier, T., Churcher, C., Harris, D., Gordon, S. V., Eiglmeier, K., Gas, S., Barry, C. E., Tekaia, F., Badcock, K., Basham, D., Brown, D., Chillingworth, T., Conner, R., Davies, R., Devlin, K., Feltwell, T., Gentles, S., Hamlin, N., Holroyd, S., Hornsby, T., Jagels, K., Krogh, A., McLean, J., Moule, S., Murphy, L., Oliver, K., Osborne, J., Quail, M. A., Rajandream, M. A., Rogers, J., Rutter, S., Seeger, K., Skelton, J., Squares, R., Squares, S., Sulston, J. E., Taylor, K., Whitehead, S., and Barrell, B. G. (1998) Deciphering the biology of Mycobacterium tuberculosis from the complete genome sequence (vol 393, pg 537, 1998), *Nature 396*, 190-198.
14. Gatfield, J., and Pieters, J. (2000) Essential role for cholesterol in entry of mycobacteria into macrophages, *Science 288*, 1647-1650.
15. Pandey, A. K., and Sassetti, C. M. (2008) Mycobacterial persistence requires the utilization of host cholesterol, *Proc Natl Acad Sci U S A 105*, 4376-4380.
16. van der Wel, N., Hava, D., Houben, D., Fluitsma, D., van Zon, M., Pierson, J., Brenner, M., and Peters, P. J. (2007) M. tuberculosis and M. leprae translocate from the phagolysosome to the cytosol in myeloid cells, *Cell 129*, 1287-1298.
17. Donova, M. V. (2007) [Transformation of steroids by actinobacteria: a review], *Prikladnaia biokhimiia i mikrobiologiia 43*, 5-18.
18. van der Geize, R., Hessels, G. I., van Gerwen, R., van der Meijden, P., and Dijkhuizen, L. (2002) Molecular and functional characterization of kshA and

kshB, encoding two components of 3-ketosteroid 9alpha-hydroxylase, a class IA monooxygenase, in Rhodococcus erythropolis strain SQ1, *Molecular microbiology 45*, 1007-1018.

19. Horinouchi, M., Kurita, T., Yamamoto, T., Hatori, E., Hayashi, T., and Kudo, T. (2004) Steroid degradation gene cluster of Comamonas testosteroni consisting of 18 putative genes from meta-cleavage enzyme gene tesB to regulator gene tesR, *Biochemical and biophysical research communications 324*, 597-604.
20. Horinouchi, M., Hayashi, T., Koshino, H., Kurita, T., and Kudo, T. (2005) Identification of 9,17-dioxo-1,2,3,4,10,19-hexanorandrostan-5-oic acid, 4-hydroxy-2-oxohexanoic acid, and 2-hydroxyhexa-2,4-dienoic acid and related enzymes involved in testosterone degradation in Comamonas testosteroni TA441, *Applied and environmental microbiology 71*, 5275-5281.
21. Andor, A., Jekkel, A., Hopwood, D. A., Jeanplong, F., Ilkoy, E., Konya, A., Kurucz, I., and Ambrus, G. (2006) Generation of useful insertionally blocked sterol degradation pathway mutants of fast-growing mycobacteria and cloning, characterization, and expression of the terminal oxygenase of the 3-ketosteroid 9alpha-hydroxylase in Mycobacterium smegmatis mc(2)155, *Applied and environmental microbiology 72*, 6554-6559.
22. van der Geize, R., Hessels, G. I., van Gerwen, R., van der Meijden, P., and Dijkhuizen, L. (2001) Unmarked gene deletion mutagenesis of kstD, encoding 3-ketosteroid Delta1-dehydrogenase, in Rhodococcus erythropolis SQ1 using sacB as counter-selectable marker, *FEMS microbiology letters 205*, 197-202.
23. van der Geize, R., Hessels, G. I., and Dijkhuizen, L. (2002) Molecular and functional characterization of the kstD2 gene of Rhodococcus erythropolis SQ1 encoding a second 3-ketosteroid Delta(1)-dehydrogenase isoenzyme, *Microbiology (Reading, England) 148*, 3285-3292.
24. Brzostek, A., Sliwinski, T., Rumijowska-Galewicz, A., Korycka-Machala, M., and Dziadek, J. (2005) Identification and targeted disruption of the gene encoding the main 3-ketosteroid dehydrogenase in Mycobacterium smegmatis, *Microbiology (Reading, England) 151*, 2393-2402.
25. Gibson, D. T., Wang, K. C., Sih, C. J., and Whitlock, H., Jr. (1966) Mechanisms of steroid oxidation by microorganisms. IX. On the mechanism of ring A cleavage in the degradation of 9,10-seco steroids by microorganisms, *The Journal of biological chemistry 241*, 551-559.
26. Owen, R. W., Mason, A. N., and Bilton, R. F. (1983) The degradation of cholesterol by Pseudomonas sp. NCIB 10590 under aerobic conditions, *J Lipid Res 24*, 1500-1511.
27. Jain, M., Petzold, C. J., Schelle, M. W., Leavell, M. D., Mougous, J. D., Bertozzi, C. R., Leary, J. A., and Cox, J. S. (2007) Lipidomics reveals control of Mycobacterium tuberculosis virulence lipids via metabolic coupling, *Proc Natl Acad Sci U S A 104*, 5133-5138.
28. Van der Geize, R., Yam, K., Heuser, T., Wilbrink, M. H., Hara, H., Anderton, M. C., Sim, E., Dijkhuizen, L., Davies, J. E., Mohn, W. W., and Eltis, L. D. (2007) A gene cluster encoding cholesterol catabolism in a soil actinomycete provides insight into Mycobacterium tuberculosis survival in macrophages, *Proc Natl Acad Sci U S A 104*, 1947-1952.

29. Bellamine, A., Mangla, A. T., Nes, W. D., and Waterman, M. R. (1999) Characterization and catalytic properties of the sterol 14 alpha-demethylase from Mycobacterium tuberculosis, *Proceedings of the National Academy of Sciences of the United States of America 96*, 8937-8942.
30. Yang, X., Dubnau, E., Smith, I., and Sampson, N. S. (2007) Rv1106c from Mycobacterium tuberculosis is a 3beta-hydroxysteroid dehydrogenase, *Biochemistry 46*, 9058-9067.
31. Dubnau, E., Fontan, P., Manganelli, R., Soares-Appel, S., and Smith, I. (2002) Mycobacterium tuberculosis genes induced during infection of human macrophages, *Infection and immunity 70*, 2787-2795.
32. Schnappinger, D., Ehrt, S., Voskuil, M. I., Liu, Y., Mangan, J. A., Monahan, I. M., Dolganov, G., Efron, B., Butcher, P. D., Nathan, C., and Schoolnik, G. K. (2003) Transcriptional Adaptation of Mycobacterium tuberculosis within Macrophages: Insights into the Phagosomal Environment, *The Journal of experimental medicine 198*, 693-704.
33. Purcell, J. P., Greenplate, J. T., Jennings, M. G., Ryerse, J. S., Pershing, J. C., Sims, S. R., Prinsen, M. J., Corbin, D. R., Tran, M., Sammons, R. D., and et al. (1993) Cholesterol oxidase: a potent insecticidal protein active against boll weevil larvae, *Biochemical and biophysical research communications 196*, 1406-1413.
34. Ghoshroy, K. B., Zhu, W., and Sampson, N. S. (1997) Investigation of membrane disruption in the reaction catalyzed by cholesterol oxidase, *Biochemistry 36*, 6133-6140.
35. Linder, R. (1997) Rhodococcus equi and Arcanobacterium haemolyticum: two "coryneform" bacteria increasingly recognized as agents of human infection, *Emerging infectious diseases 3*, 145-153.
36. Navas, J., Gonzalez-Zorn, B., Ladron, N., Garrido, P., and Vazquez-Boland, J. A. (2001) Identification and mutagenesis by allelic exchange of choE, encoding a cholesterol oxidase from the intracellular pathogen Rhodococcus equi, *J Bacteriol 183*, 4796-4805.
37. Pei, Y., Dupont, C., Sydor, T., Haas, A., and Prescott, J. F. (2006) Cholesterol oxidase (ChoE) is not important in the virulence of Rhodococcus equi, *Veterinary microbiology 118*, 240-246.
38. Boumpas, D. T., Chrousos, G. P., Wilder, R. L., Cupps, T. R., and Balow, J. E. (1993) Glucocorticoid therapy for immune-mediated diseases: basic and clinical correlates, *Annals of internal medicine 119*, 1198-1208.
39. Reading, P. C., Moore, J. B., and Smith, G. L. (2003) Steroid hormone synthesis by vaccinia virus suppresses the inflammatory response to infection, *Journal of Experimental Medicine 197*, 1269-1278.
40. Asami, T., Nakano, T., and Fujioka, S. (2005) Plant brassinosteroid hormones, *Vitamins and hormones 72*, 479-504.
41. Gilbert, L. I., Rybczynski, R., and Warren, J. T. (2002) Control and biochemical nature of the ecdysteroidogenic pathway, *Annual review of entomology 47*, 883-916.

CHAPTER 2

1. Cole, S. T., Brosch, R., Parkhill, J., Garnier, T., Churcher, C., Harris, D., Gordon, S. V., Eiglmeier, K., Gas, S., Barry, C. E., Tekaia, F., Badcock, K., Basham, D., Brown, D., Chillingworth, T., Conner, R., Davies, R., Devlin, K., Feltwell, T., Gentles, S., Hamlin, N., Holroyd, S., Hornsby, T., Jagels, K., Krogh, A., McLean, J., Moule, S., Murphy, L., Oliver, K., Osborne, J., Quail, M. A., Rajandream, M. A., Rogers, J., Rutter, S., Seeger, K., Skelton, J., Squares, R., Squares, S., Sulston, J. E., Taylor, K., Whitehead, S., and Barrell, B. G. (1998) Deciphering the biology of Mycobacterium tuberculosis from the complete genome sequence (vol 393, pg 537, 1998), *Nature 396*, 190-198.
2. Boumpas, D. T., Chrousos, G. P., Wilder, R. L., Cupps, T. R., and Balow, J. E. (1993) Glucocorticoid therapy for immune-mediated diseases: basic and clinical correlates, *Annals of internal medicine 119*, 1198-1208.
3. Reading, P. C., Moore, J. B., and Smith, G. L. (2003) Steroid hormone synthesis by vaccinia virus suppresses the inflammatory response to infection, *Journal of Experimental Medicine 197*, 1269-1278.
4. Yang, X., Dubnau, E., Smith, I., and Sampson, N. S. (2007) Rv1106c from Mycobacterium tuberculosis is a 3beta-hydroxysteroid dehydrogenase, *Biochemistry 46*, 9058-9067.
5. Nagano, S., Cupp-Vickery, J. R., and Poulos, T. L. (2005) Crystal structures of the ferrous dioxygen complex of wild-type cytochrome P450eryF and its mutants, A245S and A245T - Investigation of the proton transfer system in P450eryF, *Journal of Biological Chemistry 280*, 22102-22107.
6. Warman, A. J., Roitel, O., Neeli, R., Girvan, H. M., Seward, H. E., Murray, S. A., McLean, K. J., Joyce, M. G., Toogood, H., Holt, R. A., Leys, D., Scrutton, N. S., and Munro, A. W. (2005) Flavocytochrome P450 BM3: an update on structure and mechanism of a biotechnologically important enzyme, *Biochemical Society transactions 33*, 747-753.
7. Bentley, S. D., Chater, K. F., Cerdeno-Tarraga, A. M., Challis, G. L., Thomson, N. R., James, K. D., Harris, D. E., Quail, M. A., Kieser, H., Harper, D., Bateman, A., Brown, S., Chandra, G., Chen, C. W., Collins, M., Cronin, A., Fraser, A., Goble, A., Hidalgo, J., Hornsby, T., Howarth, S., Huang, C. H., Kieser, T., Larke, L., Murphy, L., Oliver, K., O'Neil, S., Rabbinowitsch, E., Rajandream, M. A., Rutherford, K., Rutter, S., Seeger, K., Saunders, D., Sharp, S., Squares, R., Squares, S., Taylor, K., Warren, T., Wietzorrek, A., Woodward, J., Barrell, B. G., Parkhill, J., and Hopwood, D. A. (2002) Complete genome sequence of the model actinomycete Streptomyces coelicolor A3(2), *Nature 417*, 141-147.
8. Garnier, T., Eiglmeier, K., Camus, J. C., Medina, N., Mansoor, H., Pryor, M., Duthoy, S., Grondin, S., Lacroix, C., Monsempe, C., Simon, S., Harris, B., Atkin, R., Doggett, J., Mayes, R., Keating, L., Wheeler, P. R., Parkhill, J., Barrell, B. G., Cole, S. T., Gordon, S. V., and Hewinson, R. G. (2003) The complete genome sequence of Mycobacterium bovis, *Proc Natl Acad Sci U S A 100*, 7877-7882.
9. Blattner, F. R., Plunkett, G., 3rd, Bloch, C. A., Perna, N. T., Burland, V., Riley, M., Collado-Vides, J., Glasner, J. D., Rode, C. K., Mayhew, G. F., Gregor, J., Davis, N. W., Kirkpatrick, H. A., Goeden, M. A., Rose, D. J., Mau, B., and Shao,

Y. (1997) The complete genome sequence of Escherichia coli K-12, *Science 277*, 1453-1474.

10. Venter, J. C., Adams, M. D., Myers, E. W., Li, P. W., Mural, R. J., Sutton, G. G., Smith, H. O., Yandell, M., Evans, C. A., Holt, R. A., Gocayne, J. D., Amanatides, P., Ballew, R. M., Huson, D. H., Wortman, J. R., Zhang, Q., Kodira, C. D., Zheng, X. Q. H., Chen, L., Skupski, M., Subramanian, G., Thomas, P. D., Zhang, J. H., Miklos, G. L. G., Nelson, C., Broder, S., Clark, A. G., Nadeau, C., McKusick, V. A., Zinder, N., Levine, A. J., Roberts, R. J., Simon, M., Slayman, C., Hunkapiller, M., Bolanos, R., Delcher, A., Dew, I., Fasulo, D., Flanigan, M., Florea, L., Halpern, A., Hannenhalli, S., Kravitz, S., Levy, S., Mobarry, C., Reinert, K., Remington, K., Abu-Threideh, J., Beasley, E., Biddick, K., Bonazzi, V., Brandon, R., Cargill, M., Chandramouliswaran, I., Charlab, R., Chaturvedi, K., Deng, Z. M., Di Francesco, V., Dunn, P., Eilbeck, K., Evangelista, C., Gabrielian, A. E., Gan, W., Ge, W. M., Gong, F. C., Gu, Z. P., Guan, P., Heiman, T. J., Higgins, M. E., Ji, R. R., Ke, Z. X., Ketchum, K. A., Lai, Z. W., Lei, Y. D., Li, Z. Y., Li, J. Y., Liang, Y., Lin, X. Y., Lu, F., Merkulov, G. V., Milshina, N., Moore, H. M., Naik, A. K., Narayan, V. A., Neelam, B., Nusskern, D., Rusch, D. B., Salzberg, S., Shao, W., Shue, B. X., Sun, J. T., Wang, Z. Y., Wang, A. H., Wang, X., Wang, J., Wei, M. H., Wides, R., Xiao, C. L., Yan, C. H., Yao, A., Ye, J., Zhan, M., Zhang, W. Q., Zhang, H. Y., Zhao, Q., Zheng, L. S., Zhong, F., Zhong, W. Y., Zhu, S. P. C., Zhao, S. Y., Gilbert, D., Baumhueter, S., Spier, G., Carter, C., Cravchik, A., Woodage, T., Ali, F., An, H. J., Awe, A., Baldwin, D., Baden, H., Barnstead, M., Barrow, I., Beeson, K., Busam, D., Carver, A., Center, A., Cheng, M. L., Curry, L., Danaher, S., Davenport, L., Desilets, R., Dietz, S., Dodson, K., Doup, L., Ferriera, S., Garg, N., Gluecksmann, A., Hart, B., Haynes, J., Haynes, C., Heiner, C., Hladun, S., Hostin, D., Houck, J., Howland, T., Ibegwam, C., Johnson, J., Kalush, F., Kline, L., Koduru, S., Love, A., Mann, F., May, D., McCawley, S., McIntosh, T., McMullen, I., Moy, M., Moy, L., Murphy, B., Nelson, K., Pfannkoch, C., Pratts, E., Puri, V., Qureshi, H., Reardon, M., Rodriguez, R., Rogers, Y. H., Romblad, D., Ruhfel, B., Scott, R., Sitter, C., Smallwood, M., Stewart, E., Strong, R., Suh, E., Thomas, R., Tint, N. N., Tse, S., Vech, C., Wang, G., Wetter, J., Williams, S., Williams, M., Windsor, S., Winn-Deen, E., Wolfe, K., Zaveri, J., Zaveri, K., Abril, J. F., Guigo, R., Campbell, M. J., Sjolander, K. V., Karlak, B., Kejariwal, A., Mi, H. Y., Lazareva, B., Hatton, T., Narechania, A., Diemer, K., Muruganujan, A., Guo, N., Sato, S., Bafna, V., Istrail, S., Lippert, R., Schwartz, R., Walenz, B., Yooseph, S., Allen, D., Basu, A., Baxendale, J., Blick, L., Caminha, M., Carnes-Stine, J., Caulk, P., Chiang, Y. H., Coyne, M., Dahlke, C., Mays, A. D., Dombroski, M., Donnelly, M., Ely, D., Esparham, S., Fosler, C., Gire, H., Glanowski, S., Glasser, K., Glodek, A., Gorokhov, M., Graham, K., Gropman, B., Harris, M., Heil, J., Henderson, S., Hoover, J., Jennings, D., Jordan, C., Jordan, J., Kasha, J., Kagan, L., Kraft, C., Levitsky, A., Lewis, M., Liu, X. J., Lopez, J., Ma, D., Majoros, W., McDaniel, J., Murphy, S., Newman, M., Nguyen, T., Nguyen, N., Nodell, M., Pan, S., Peck, J., Peterson, M., Rowe, W., Sanders, R., Scott, J., Simpson, M., Smith, T., Sprague, A., Stockwell, T., Turner, R., Venter, E., Wang, M., Wen, M. Y., Wu, D., Wu, M., Xia, A., Zandieh, A., and Zhu, X. H. (2001) The sequence of the human genome, *Science 291*, 1304-+.

11. Bellamine, A., Mangla, A. T., Nes, W. D., and Waterman, M. R. (1999) Characterization and catalytic properties of the sterol 14 alpha-demethylase from Mycobacterium tuberculosis, *Proceedings of the National Academy of Sciences of the United States of America 96*, 8937-8942.
12. Podust, L. M., Poulos, T. L., and Waterman, M. R. (2001) Crystal structure of cytochrome P450 14 alpha-sterol demethylase (CYP51) from Mycobacterium tuberculosis in complex with azole inhibitors, *Proceedings of the National Academy of Sciences of the United States of America 98*, 3068-3073.
13. Podust, L. M., Poulos, T. L., and Waterman, M. R. (2001) Crystal structure of cytochrome P450 14alpha -sterol demethylase (CYP51) from Mycobacterium tuberculosis in complex with azole inhibitors, *Proc Natl Acad Sci U S A 98*, 3068-3073.
14. Hishiki, T., Shimada, H., Nagano, S., Egawa, T., Kanamori, Y., Makino, R., Park, S. Y., Adachi, S., Shiro, Y., and Ishimura, Y. (2000) X-ray crystal structure and catalytic properties of Thr252Ile mutant of cytochrome P450cam: roles of Thr252 and water in the active center, *Journal of biochemistry 128*, 965-974.
15. Girvan, H. M., Marshall, K. R., Lawson, R. J., Leys, D., Joyce, M. G., Clarkson, J., Smith, W. E., Cheesman, M. R., and Munro, A. W. (2004) Flavocytochrome P450 BM3 mutant A264E undergoes substrate-dependent formation of a novel heme iron ligand set, *The Journal of biological chemistry 279*, 23274-23286.
16. Bellamine, A., Mangla, A. T., Nes, W. D., and Waterman, M. R. (1999) Characterization and catalytic properties of the sterol 14alpha-demethylase from Mycobacterium tuberculosis, *Proc Natl Acad Sci U S A 96*, 8937-8942.
17. Odds, F. C., Brown, A. J., and Gow, N. A. (2003) Antifungal agents: mechanisms of action, *Trends Microbiol 11*, 272-279.
18. McLean, K. J., Cheesman, M. R., Rivers, S. L., Richmond, A., Leys, D., Chapman, S. K., Reid, G. A., Price, N. C., Kelly, S. M., Clarkson, J., Smith, W. E., and Munro, A. W. (2002) Expression, purification and spectroscopic characterization of the cytochrome P450CYP121 from Mycobacterium tuberculosis, *Journal of Inorganic Biochemistry 91*, 527-541.
19. Leys, D., Mowat, C. G., McLean, K. J., Richmond, A., Chapman, S. K., Walkinshaw, M. D., and Munro, A. W. (2003) Atomic structure of Mycobacterium tuberculosis CYP121 to 1.06 A reveals novel features of cytochrome P450, *The Journal of biological chemistry 278*, 5141-5147.
20. Ouellet, H., Podust, L. M., and de Montellano, P. R. (2008) Mycobacterium tuberculosis CYP130: crystal structure, biophysical characterization, and interactions with antifungal azole drugs, *The Journal of biological chemistry 283*, 5069-5080.
21. Schnappinger, D., Ehrt, S., Voskuil, M. I., Liu, Y., Mangan, J. A., Monahan, I. M., Dolganov, G., Efron, B., Butcher, P. D., Nathan, C., and Schoolnik, G. K. (2003) Transcriptional adaptation of Mycobacterium tuberculosis within macrophages: Insights into the phagosomal environment, *Journal of Experimental Medicine 198*, 693-704.
22. Rengarajan, J., Bloom, B. R., and Rubin, E. J. (2005) Genome-wide requirements for Mycobacterium tuberculosis adaptation and survival in macrophages, *Proc Natl Acad Sci U S A 102*, 8327-8332.

23. Chang, J. C., Harik, N. S., Liao, R. P., and Sherman, D. R. (2007) Identification of Mycobacterial genes that alter growth and pathology in macrophages and in mice, *The Journal of infectious diseases 196*, 788-795.
24. Seward, H. E., Roujeinikova, A., McLean, K. J., Munro, A. W., and Leys, D. (2006) Crystal structure of the Mycobacterium tuberculosis P450 CYP121-fluconazole complex reveals new azole drug-P450 binding mode, *The Journal of biological chemistry 281*, 39437-39443.
25. Gamieldien, J., Ptitsyn, A., and Hide, W. (2002) Eukaryotic genes in Mycobacterium tuberculosis could have a role in pathogenesis and immunomodulation, *Trends Genet 18*, 5-8.
26. Stewart, G. R., Wernisch, L., Stabler, R., Mangan, J. A., Hinds, J., Laing, K. G., Young, D. B., and Butcher, P. D. (2002) Dissection of the heat-shock response in Mycobacterium tuberculosis using mutants and microarrays, *Microbiology (Reading, England) 148*, 3129-3138.
27. Kendall, S. L., Rison, S. C., Movahedzadeh, F., Frita, R., and Stoker, N. G. (2004) What do microarrays really tell us about M. tuberculosis?, *Trends Microbiol 12*, 537-544.
28. Sassetti, C. M., Boyd, D. H., and Rubin, E. J. (2003) Genes required for mycobacterial growth defined by high density mutagenesis, *Molecular microbiology 48*, 77-84.
29. Recchi, C., Sclavi, B., Rauzier, J., Gicquel, B., and Reyrat, J. M. (2003) Mycobacterium tuberculosis Rv1395 is a class III transcriptional regulator of the AraC family involved in cytochrome P450 regulation, *The Journal of biological chemistry 278*, 33763-33773.
30. McLean, K. J., Dunford, A. J., Neeli, R., Driscoll, M. D., and Munro, A. W. (2007) Structure, function and drug targeting in Mycobacterium tuberculosis cytochrome P450 systems, *Archives of biochemistry and biophysics 464*, 228-240.
31. Podust, L. M., von Kries, J. P., Eddine, A. N., Kim, Y., Yermalitskaya, L. V., Kuehne, R., Ouellet, H., Warrier, T., Altekoster, M., Lee, J. S., Rademann, J., Oschkinat, H., Kaufmann, S. H., and Waterman, M. R. (2007) Small-molecule scaffolds for CYP51 inhibitors identified by high-throughput screening and defined by X-ray crystallography, *Antimicrobial agents and chemotherapy 51*, 3915-3923.
32. McLean, K. J., Dunford, A. J., Sabri, M., Neeli, R., Girvan, H. M., Balding, P. R., Leys, D., Seward, H. E., Marshall, K. R., and Munro, A. W. (2006) CYP121, CYP51 and associated redox systems in Mycobacterium tuberculosis: towards deconvoluting enzymology of P450 systems in a human pathogen, *Biochemical Society transactions 34*, 1178-1182.

CHAPTER 3

1. Turfitt, G. E. (1944) The microbiological degradation of steroids: 2. Oxidation of cholesterol by Proactinomyces spp, *The Biochemical journal 38*, 492-496.
2. Sih, C. J., Tai, H. H., and Tsong, Y. Y. (1967) The mechanism of microbial conversion of cholesterol into 17-keto steroids, *J Am Chem Soc 89*, 1957-1958.
3. Bjorkhem, I., and Gustafsson, J. A. (1971) Mechanism of microbial transformation of cholesterol into coprostanol, *European journal of biochemistry / FEBS 21*, 428-432.
4. Uwajima, T., Yagi, H., Nakamura, S., and Terada, O. (1973) Isolation and Crystallization of Extracellular 3beta-Hydroxysteroid Oxidase of Brevibacterium-Sterolicum Nov-Sp, *Agricultural and Biological Chemistry 37*, 2345-2350.
5. Richmond, W. (1972) The development of an enzymatic technique for the assay of cholesterol in biological fluids, *Scandinavian journal of clinical and laboratory investigation 29*, 25.
6. Flegg, H. M. (1973) An investigation of the determination of serum cholesterol by an enzymic method, *Annals of Clinical Biochemistry 10*, 79-84.
7. Richmond, W. (1973) Preparation and properties of a cholesterol oxidase from Nocardia sp. and its application to the enzymatic assay of total cholesterol in serum, *Clinical chemistry 19*, 1350-1356.
8. el Yandouzi, E. H., and Le Grimellec, C. (1992) Cholesterol heterogeneity in the plasma membrane of epithelial cells, *Biochemistry 31*, 547-551.
9. Lange, Y. (1992) Tracking Cell Cholesterol with Cholesterol Oxidase, *Journal of Lipid Research 33*, 315-319.
10. Lange, Y., Matthies, H., and Steck, T. L. (1984) Cholesterol oxidase susceptibility of the red cell membrane, *Biochimica et biophysica acta 769*, 551-562.
11. Lange, Y., and Steck, T. L. (1996) The role of intracellular cholesterol transport in cholesterol homeostasis, *Trends in cell biology 6*, 205-208.
12. Lange, Y., Ye, J., and Steck, T. L. (2005) Activation of membrane cholesterol by displacement from phospholipids, *The Journal of biological chemistry 280*, 36126-36131.
13. London, E. (2002) Insights into lipid raft structure and formation from experiments in model membranes, *Current opinion in structural biology 12*, 480-486.
14. Gadda, G., Wels, G., Pollegioni, L., Zucchelli, S., Ambrosius, D., Pilone, M. S., and Ghisla, S. (1997) Characterization of cholesterol oxidase from Streptomyces hygroscopicus and Brevibacterium sterolicum, *European Journal of Biochemistry 250*, 369-376.
15. Vrielink, A., Lloyd, L. F., and Blow, D. M. (1991) Crystal structure of cholesterol oxidase from Brevibacterium sterolicum refined at 1.8 A resolution, *J Mol Biol 219*, 533-554.
16. Li, J., Vrielink, A., Brick, P., and Blow, D. M. (1993) Crystal structure of cholesterol oxidase complexed with a steroid substrate: implications for flavin adenine dinucleotide dependent alcohol oxidases, *Biochemistry 32*, 11507-11515.
17. Yue, Q. K., Kass, I. J., Sampson, N. S., and Vrielink, A. (1999) Crystal structure determination of cholesterol oxidase from Streptomyces and structural characterization of key active site mutants, *Biochemistry 38*, 4277-4286.

18. Cavener, D. R. (1992) GMC oxidoreductases. A newly defined family of homologous proteins with diverse catalytic activities, *J Mol Biol 223*, 811-814.
19. Kass, I. J., and Sampson, N. S. (1998) Evaluation of the role of His447 in the reaction catalyzed by cholesterol oxidase, *Biochemistry 37*, 17990-18000.
20. Lario, P. I., Sampson, N., and Vrielink, A. (2003) Sub-atomic resolution crystal structure of cholesterol oxidase: what atomic resolution crystallography reveals about enzyme mechanism and the role of the FAD cofactor in redox activity, *J Mol Biol 326*, 1635-1650.
21. Kass, I. J., and Sampson, N. S. (1995) The isomerization catalyzed by Brevibacterium sterolicum cholesterol oxidase proceeds stereospecifically with one base, *Biochemical and biophysical research communications 206*, 688-693.
22. Sampson, N. S., and Kass, I. J. (1997) Isomerization, but not oxidation, is suppressed by a single point mutation, E361Q, in the reaction catalyzed by cholesterol oxidase, *Journal of the American Chemical Society 119*, 855-862.
23. Kass, I. J., and Sampson, N. S. (1998) The importance of GLU361 position in the reaction catalyzed by cholesterol oxidase, *Bioorganic & medicinal chemistry letters 8*, 2663-2668.
24. Yin, Y., Sampson, N. S., Vrielink, A., and Lario, P. I. (2001) The presence of a hydrogen bond between asparagine 485 and the pi system of FAD modulates the redox potential in the reaction catalyzed by cholesterol oxidase, *Biochemistry 40*, 13779-13787.
25. Gadda, G., Wels, G., Pollegioni, L., Zucchelli, S., Ambrosius, D., Pilone, M. S., and Ghisla, S. (1997) Characterization of cholesterol oxidase from Streptomyces hygroscopicus and Brevibacterium sterolicum, *European journal of biochemistry / FEBS 250*, 369-376.
26. Coulombe, R., Yue, K. Q., Ghisla, S., and Vrielink, A. (2001) Oxygen access to the active site of cholesterol oxidase through a narrow channel is gated by an Arg-Glu pair, *The Journal of biological chemistry 276*, 30435-30441.
27. Motteran, L., Pilone, M. S., Molla, G., Ghisla, S., and Pollegioni, L. (2001) Cholesterol oxidase from Brevibacterium sterolicum. The relationship between covalent flavinylation and redox properties, *The Journal of biological chemistry 276*, 18024-18030.

CHAPTER 4

1. Kempf, J. G., and Loria, J. P. (2003) Protein dynamics from solution NMR - Theory and applications, *Cell Biochemistry and Biophysics 37*, 187-211.
2. Szyperski, T., Luginbuhl, P., Otting, G., Guntert, P., and Wuthrich, K. (1993) Protein Dynamics Studied by Rotating Frame N-15 Spin Relaxation-Times, *Journal of Biomolecular Nmr 3*, 151-164.
3. Akke, M., and Palmer, A. G. (1996) Monitoring macromolecular motions on microsecond to millisecond time scales by R(1)rho-R(1) constant relaxation time NMR spectroscopy, *Journal of the American Chemical Society 118*, 911-912.
4. Kempf, J. G., Jung, J. Y., Sampson, N. S., and Loria, J. P. (2003) Off-resonance TROSY (R-1 rho-R-1) for quantitation of fast exchange processes in large proteins, *Journal of the American Chemical Society 125*, 12064-12065.
5. Nomura, N., Choi, K. P., Yamashita, M., Yamamoto, H., and Murooka, Y. (1995) Genetic-Modification of the Streptomyces Cholesterol Oxidase Gene for Expression in Escherichia-Coli and Development of Promoter-Probe Vectors for Use in Enteric Bacteria, *Journal of Fermentation and Bioengineering 79*, 410-416.
6. Vogel, H. J. (2002) *Calcium-Binding Protein Protocols: Methods and Techniques*, Humana Press.
7. Sampson, N. S., Kass, I. J., and Ghoshroy, K. B. (1998) Assessment of the role of an omega loop of cholesterol oxidase: a truncated loop mutant has altered substrate specificity, *Biochemistry 37*, 5770-5778.

Appendix

I-1. Plasmid containing N-terminal his-tagged *cyp125* (a gift from Astra Zeneca, in pET28a)

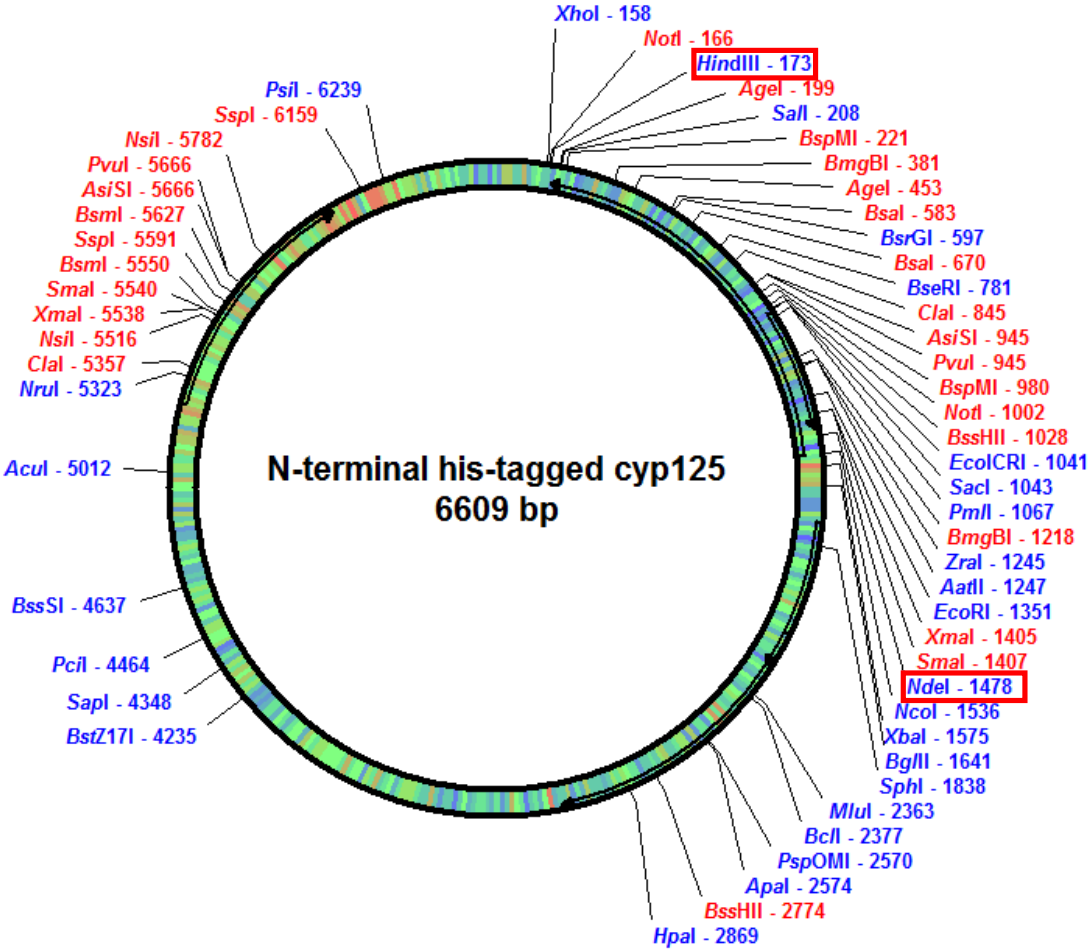

I-2. Plasmid containing C-terminal his-tagged *cyp125* (in pET20b)

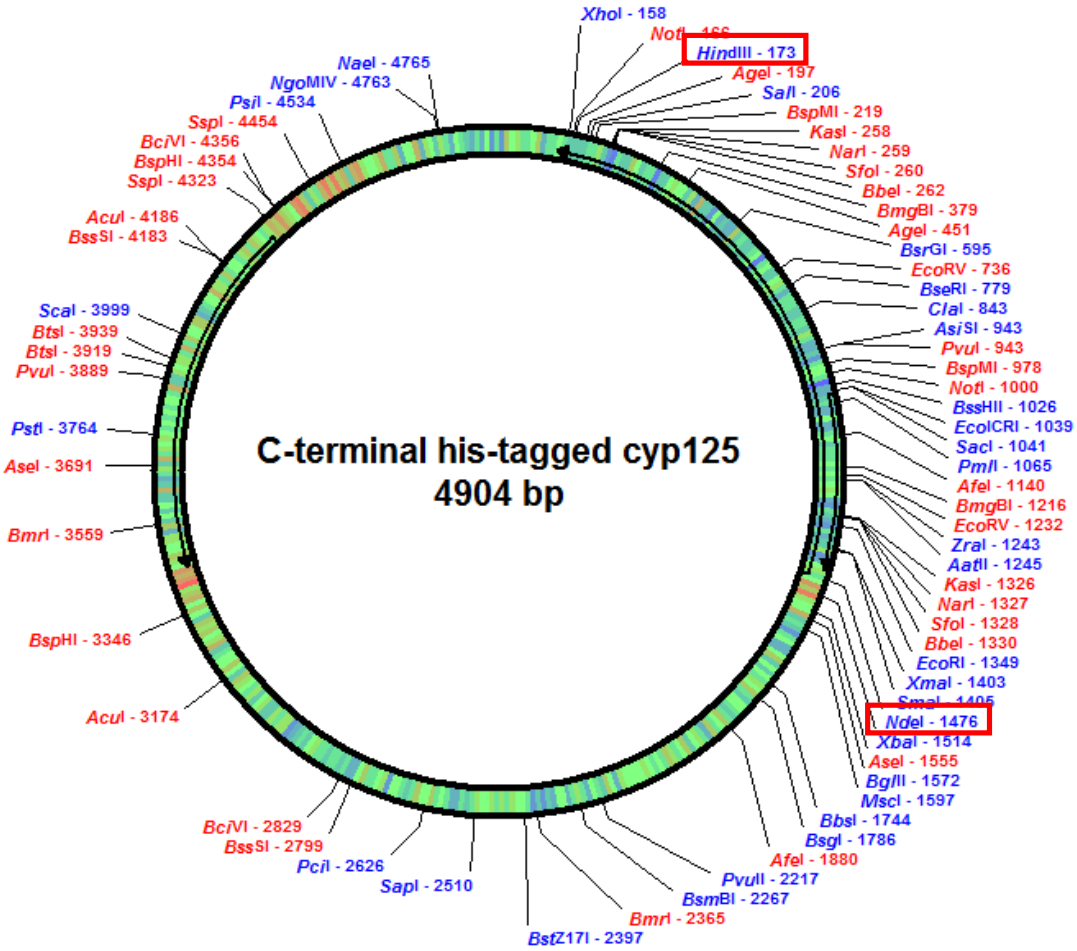

I-3. Plasmid containing N/C-terminal his-tagged *cyp125* (in pET28b)

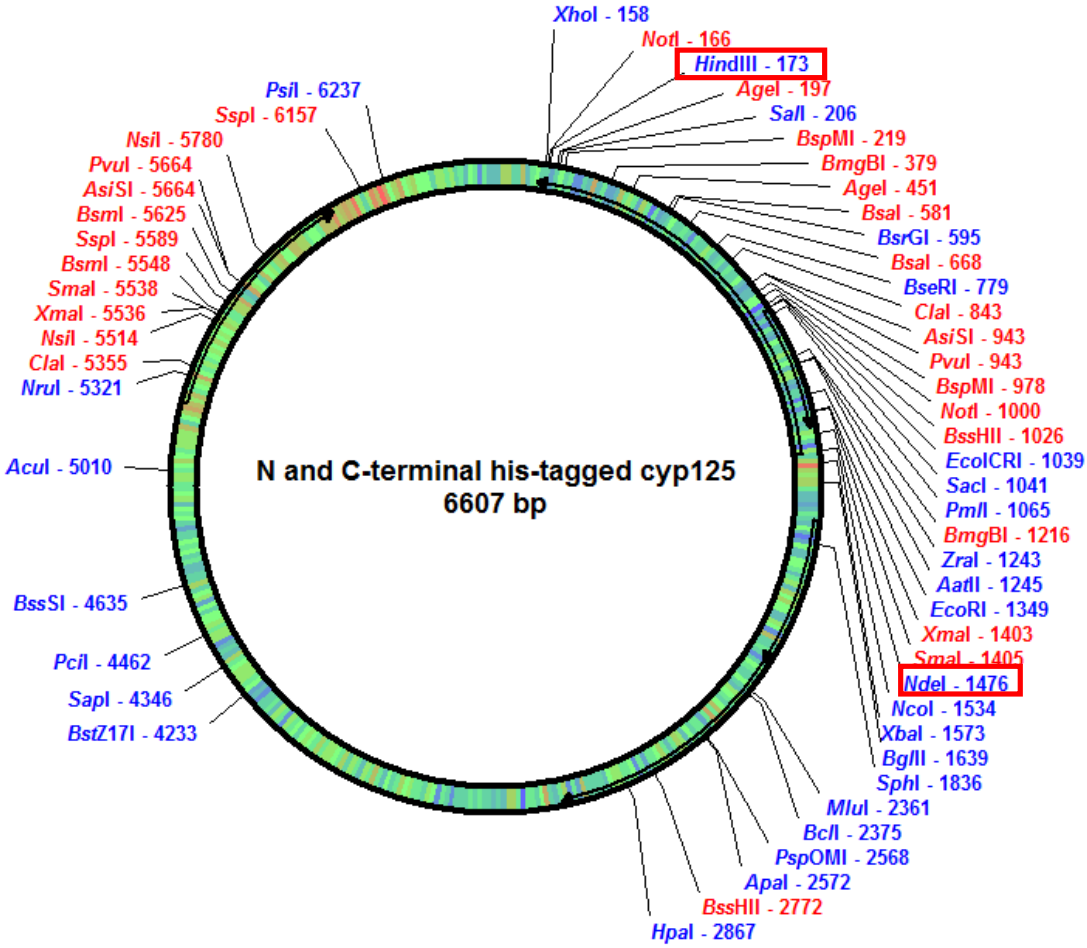

I-4. Plasmid containing C-terminal his-tagged *cyp121* (in pET29a)

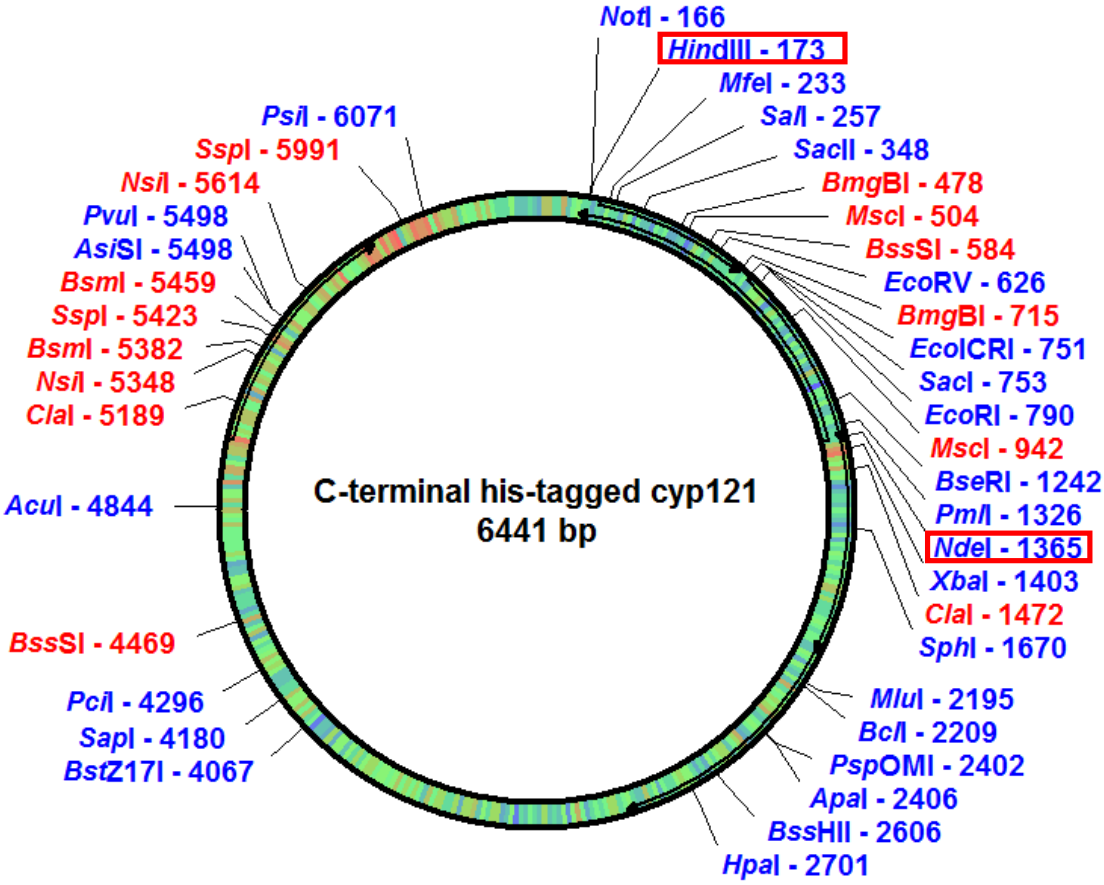

I-5. Plasmid containing C-terminal his-tagged *cyp125* (in pVV16)

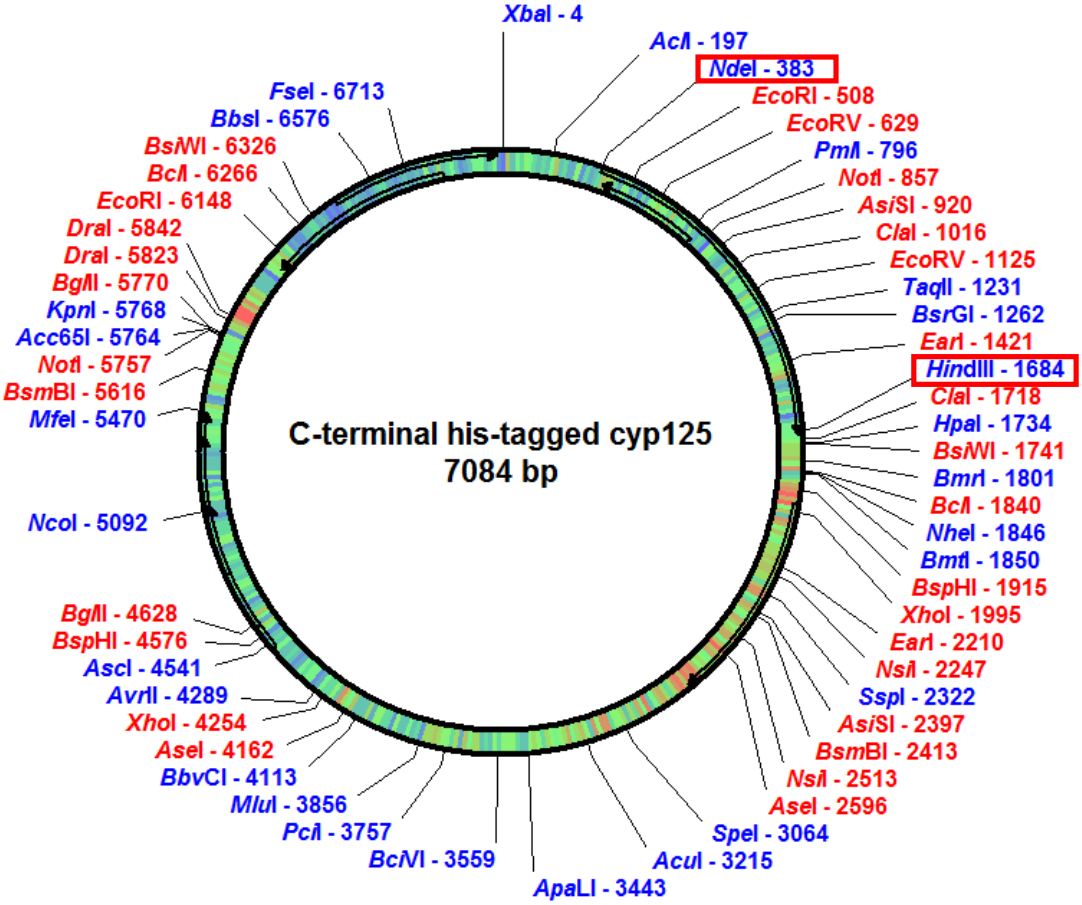

I-6. Plasmid pCO202

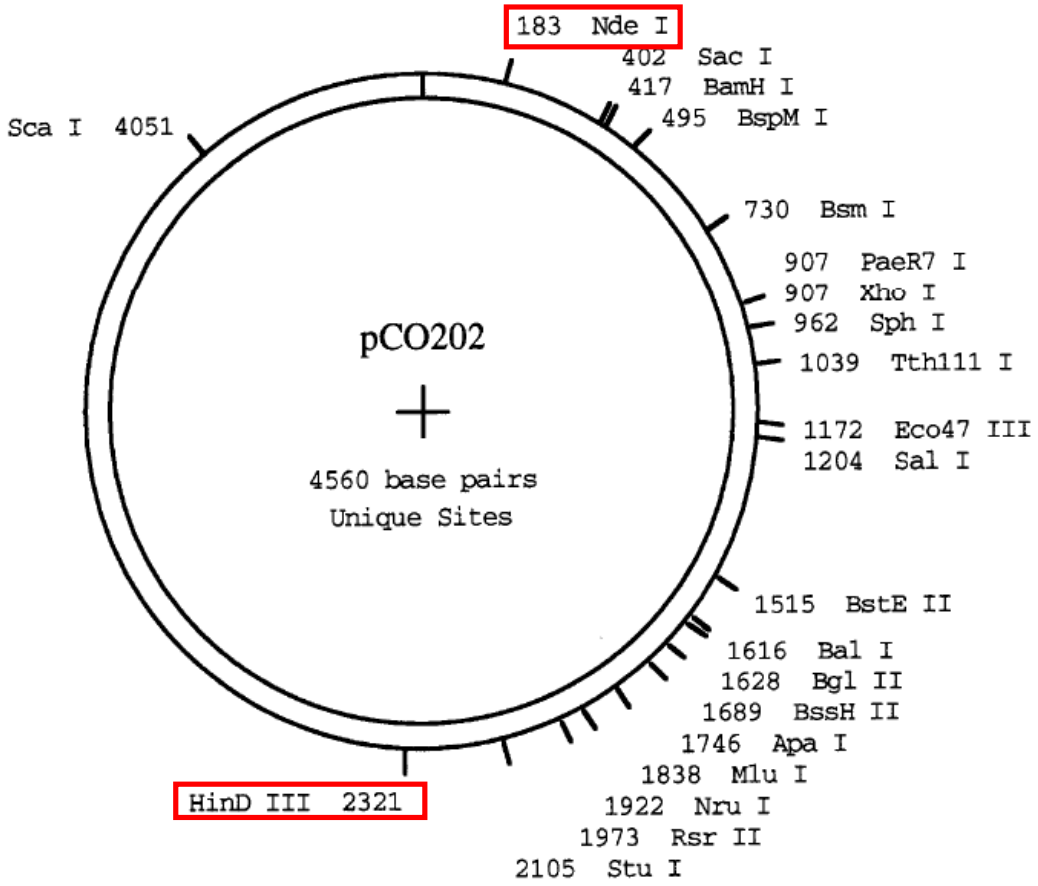

I-7. Plasmid pCO117